Southeastern Geology: Volume 45, No. 1 June 2007

Editor in Chief: S. Duncan Heron, Jr.

Abstract

Academic journal published quarterly by the Department of Geology, Duke University.

SOUTHEASTERN GEOLOGY

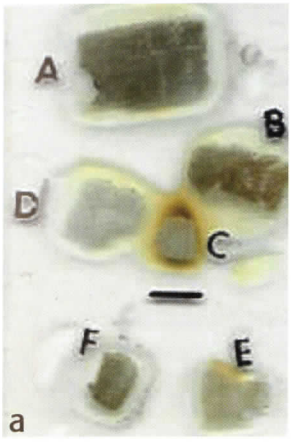

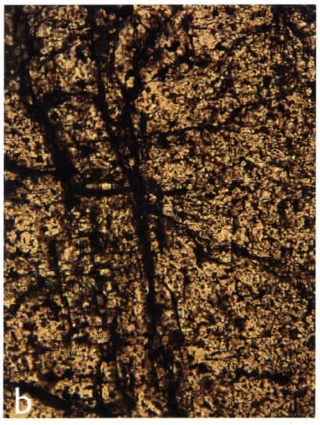

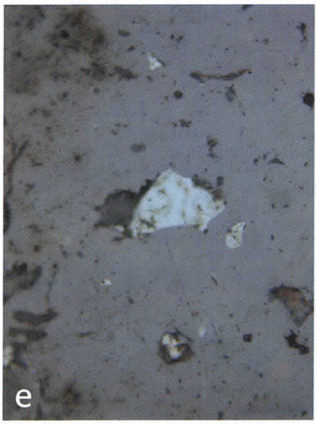

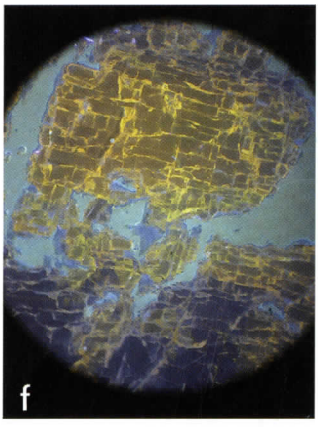

Vol. 45, No. 1 June 2007

SOUTHEASTERN GEOLOGY

PUBLISHED

at

DUKE UNIVERSITY

Duncan Heron

Editor in Chief

David M. Bush

Editor

This journal publishes the results of original research on all phases of geology, geophysics, geochemistry and environmental geology as related to the Southeast. Send manuscripts to **David Bush, Department of Geosciences, University of West Georgia, Carrollton, Georgia 30118, for Fed-X, etc. 1601 Maple St.,** Phone: 678-839-4057, Fax: 678-839-4071, Email: dbush@westga.edu. Please observe the following:

1) Type the manuscript with double space lines and submit in duplicate, or submit as an Acrobat file attached to an email.
2) Cite references and prepare bibliographic lists in accordance with the method found within the pages of this journal. Data citations examples can be found at http://www.geoinfo.org/TFGeosciData.htm
3) Submit line drawings and complex tables reduced to final publication size (no bigger than 8 x 5 3/8 inches).
4) Make certain that all photographs are sharp, clear, and of good contrast.
5) Stratigraphic terminology should abide by the North American Stratigraphic Code (American Association Petroleum Geologists Bulletin, v. 67, p. 841-875).
6) Email Acrobat (pdf) submissions are encouraged.

Subscriptions to *Southeastern Geology* for volume 45 are: individuals - $24.00 (paid by personal check); corporations and libraries - $36.00; foreign $48. Inquires should be sent to: **SOUTHEASTERN GEOLOGY, DUKE UNIVERSITY, DIVISION OF EARTH & OCEAN SCIENCES, BOX 90233, DURHAM, NORTH CAROLINA 27708-0233**. Make checks payable to: *Southeastern Geology*.

Information about **SOUTHEASTERN GEOLOGY** is on the World Wide Web including a searchable author-title index 1958-2005 (Acrobat format). The URL for the Web site is: http://www.southeasterngeology.org

SOUTHEASTERN GEOLOGY is a peer review journal.

ISSN 0038-3678

SOUTHEASTERN GEOLOGY

Table of Contents

Volume 45, No. 1 June 2007

SOUTHEASTERN GEOLOGY
V. 45, No.1, June 2007, p. 1-13

GEOCHEMISTRY OF MEGACRYSTIC ZIRCONS WITH DISTINCTIVE FLUORESCENT ZIRCON POPULATIONS FROM THE FREEMAN MINE, ZIRCONIA, NORTH CAROLINA

JOHN E. CALLAHAN[1]

Department of Geology, Appalachian State University, P.O. Box 32067 Boone, NC 28608-2067
goldjec@hotmail.com

BRENDAN R. BREAM[2]

Department of Earth and Planetary Sciences, University of Tennessee, 306 Earth and Planetary Sciences Building, Knoxville, Tennessee 37996-1410, brendan.r.bream@vanderbilt.edu

NEIL E. JOHNSON

JEFFERY D. STEPP[3]

Department of Geology, Appalachian State University, P.O. Box 32067 Boone, NC 28608-2067
johnsonne@appstate.edu

Present addresses:
[1] 783 Blairmont Dr., Boone, North Carolina 28607
[2] Department of Earth and Environmental Sciences, Vanderbilt University, Nashville, Tennessee, 37235
[3] 104 Otter Lane, Waterloo, South Carolina 29384

ABSTRACT

Megacrystic (up to 1.5 cm) euhedral to subhedral zircons occur at the Freeman Mine in a zoned syenitic pegmatite near Zirconia, North Carolina. Zircon concentrates obtained from three mine dump sites, a stream draining the dump, and nine weathered pegmatite hand samples were classified as strongly fluorescent, weakly fluorescent or non-fluorescent under shortwave ultraviolet light. Strongly fluorescent zircons in this study are pinkish gray in color, whereas weakly to non-fluorescent samples are dark pale-orange brown and tend to be coated with iron oxides that are mainly goethite with minor hematite. Zircon samples that show areas of internal mottling when viewed with a petrographic microscope, are dark pale orange brown and are not strongly fluorescent or cathodoluminescent. Small grains of magnetite (<0.1mm), very small unidentified transparent minerals (<0.05mm), and fluid inclusions (<0.01mm) are scattered throughout the zircon crystals. X-ray powder diffraction studies indicate that neither population is significantly metamict, since there are no major differences in unit cell dimensions. Average bulk chemical analyses of 0.2 gram samples of un-cleaned concentrates and cleaned concentrates indicate that weakly to non-fluorescent zircons tend to have higher average concentrations of Fe_2O_3, U, Th, Hf and total rare earth elements (REE) plus Y than the strongly fluorescent group. Electron microprobe analyses suggest that average U_2O_3 and HfO_2 values are typically higher in the weakly fluorescent samples. An inverse relationship between higher concentrations of Fe_2O_3, U, U_2O_3, Hf, HfO_2, total REE plus Y and perhaps Th, and lower fluorescence activation suggests that one or more of these trace oxides/elements — most likely Fe_2O_3, or REE — may be quenching fluorescence.

INTRODUCTION AND GEOLOGIC SETTING

This study was initiated when a difference in zircon fluorescence was noted in that some zircons from the Freeman Mine dump were fluo-

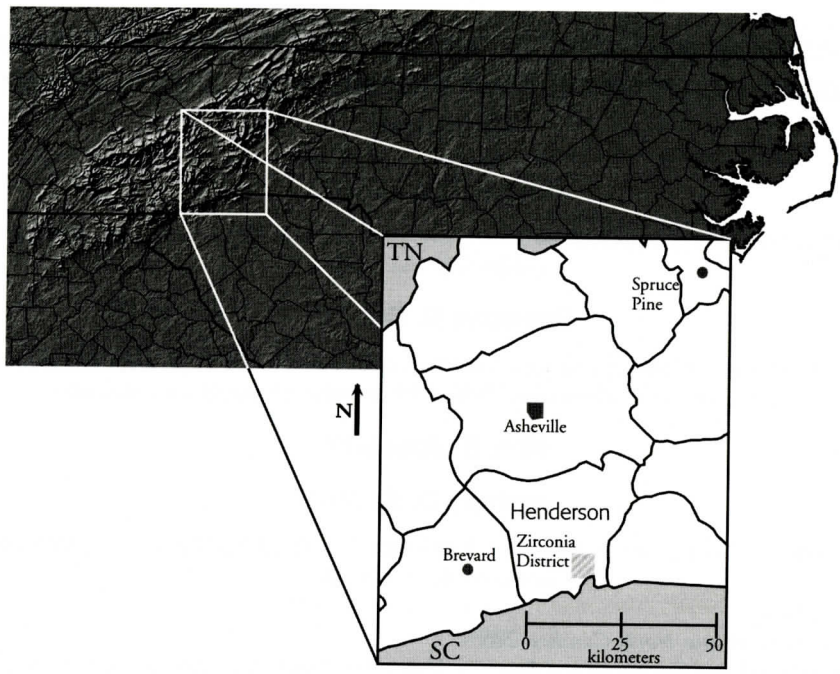

Figure 1. Location of the Zirconia District, North Carolina.

rescent and some were not. It is well known that zircons worldwide exhibit varying degrees of fluorescence, and, thus the very large zircons (megacrysts) from the Freeman site provide an opportunity to determine why some of these zircons fluoresce and some do not.

Luminescence in minerals, including fluorescence and cathodoluminescence, is the property whereby light of varying wavelengths is emitted when the sample is excited by means other than incandescent light. Quenching occurs when there is a decrease in expected or typical luminescence in minerals such as zircon. For the purposes of this paper, fluorescence is described as visible light emitted when shortwave ultraviolet light (UVL) is used to excite the sample. Cathodoluminescence (CL) is defined as light emitted from a sample when a focused electron beam is used to excite the sample. The strongly to moderately fluorescent samples in this study were given the abbreviation **SF** and the weakly fluorescent samples the abbreviation *WF*; samples that did not show fluorescence at the surface of the grain are designated as NF.

The Freeman Mine is located approximately 40 kilometers south-south east of Asheville in the western Inner Piedmont near the town of Zirconia, North Carolina (Figure 1), at 35.229°N, and 82.437°W. The Freeman Mine is included in the Zirconia District, defined by Olson (1952) as an area that encompasses an area of 14 square miles near Zirconia, North Carolina, and that includes numerous small pegmatites and the Freeman and Jones Mines. From 1869 to 1915 approximately 40 tons of zircon were obtained from the Freeman and Jones mines by pick and shovel or hydraulic methods. Mining efforts focused on weathered material to a depth of about 10-12 meters. Average zircon content of the weathered material was reported at <1% and most crystals were in the 0.1-0.25 inch range (Olson, 1952). The pit is now filled in; the mine dump is partly covered by a house, and exposures are weathered and limited.

Olson (1952) mentions that pegmatites in the area of the Freeman Mine are located within or near a large inclusion or pendant of gneiss or schist that is 0.8 to 1.6 km wide and almost 5 km long. According to Olson (1952), the pegmatites in this area are up to 70 meters long and 20-

30 meters wide. They are zoned and mainly concordant to the granitic gneiss foliation that strikes northwest and dips 20-50 degrees to the northeast, although portions of it also crosscut the gneiss. Vermiculite-rich wall zones are 4.5-6 meters thick. The border zone, within 15 cm of the contact, is composed mostly of fine-grained vermiculite, whereas the core consists mainly of pink microcline with minor vermiculite, quartz, zircon, albite, and anatase. Anatase is enriched in the inner part of the wall zone and outer part of the core. Other minerals noted from pegmatites of the Zirconia area include titanite, titaniferous garnet, polycrase, allanite, a phosphatic thorite, monazite, xenotime, epidote, stilbite, apatite, muscovite, calcite, and iron oxides (Olson, 1952).

Freeman Mine megacrystic zircons occur in a syenitic pegmatite that intrudes into the biotite quartzo-feldspathic gneiss country rock. According to a forthcoming geologic map of the Zirconia 7.5 minute quadrangle (Garihan, personal communication, 2006), the pegmatite lies in the upper Tallulah Falls Formation, about 0.5 km from and structurally above the trace of the Seneca fault. Bream (2002), correlated the Seneca fault as it is defined in South Carolina with the Sugarloaf Mountain fault defined by Davis (1993) in North Carolina. The Sugarloaf Mountain-Seneca fault is a major fault within the western Inner Piedmont, juxtaposing hanging-wall Tallulah Falls and Poor Mountain Formation rocks over footwall rocks consisting mostly of migmatitic Tallulah Falls Formation and granitoids, including the Henderson Gneiss and Caesar's Head Granite. Biotite augen gneiss samples from Bald Rock near Caesars Head State Park in South Carolina are similar to those found in the footwall of the fault near the Freeman Mine and yield Late (Ranson, et al., 1999) to Middle (Vinson, 1999) Ordovician ages. Mostly Ordovician ages have also been determined for the Henderson Gneiss (Vinson, 1999 and unpublished data (C.F. Miller and S. Meschter-McDowell). Zircons from two samples, one from Bald Rock (Table Rock Plutonic suite now referred to as the Table Rock gneiss), and one from an area approximately 8 km south southeast of the Freeman Mine, mapped as the Tallulah Falls gneiss both yielded ages of Late Ordovician (Ranson, personal communication).

SAMPLING AND ANALYTICAL METHODS

Nine weathered pegmatite samples were collected from exposures along the bank bordering a driveway, weighed, crushed with a hammer, and panned to concentrate the coarse zircons. Zircon crystals greater than 40-mesh (0.425 mm) were separated from the panned concentrates and weighed. These zircons were separated into two batches based on whether or not they fluoresced under UVL; each batch was then weighed. Zircon samples obtained from these hand specimen samples contained both fluorescent and nonfluorescent zircons in the same sample.

Mine dump material was collected in five gallon buckets, and zircon grains, greater than 40-mesh (0.425 mm) were separated by panning and sieving. The resulting grains were separated into strongly fluorescent (**SF**), weakly fluorescent (*WF*), and nonfluorescent (NF) groups using UVL. A subset of several grams of the **SF** and *WF* (**SF12-13-00**; *WF12-13-00*) grains were prepared for analyses by grinding in an agate mortar and pestle until the sample passed through a minus 80-mesh screen (0.180mm). At least two grams of sample were sent to ACME Analytical Laboratories Ltd. in Vancouver, British Columbia (ACME) for analyses of selected oxides. Later, five gallon buckets were used to collect weathered dump material at three sites and from gravel in a stream near the dump. A total of almost 36 grams of greater than 40-mesh zircons, with one crystal weighing 2 grams, was recovered from these buckets of dump material and one of stream gravel. Concentrates were separated in the same manner described above and again were divided into sets of **SF** and *WF* zircon. At least two grams of **SF** sets (samples **SF11-22-01**) and four *WF* sets (*WF11-22-01* were prepared as above and sent to ACME for bulk chemical major element, trace element and REE analysis. A final set of **SF**, *WF*, and NF from the stream gravel was concentrated and

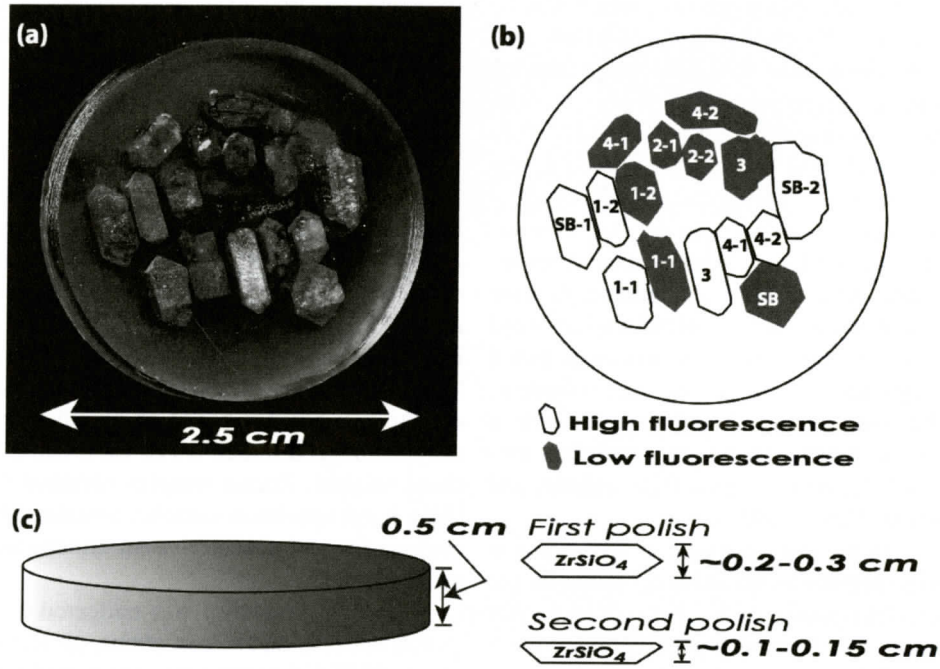

Figure 2. Grain mount prepared for SHRIMP-RG (Bream, 2003) and electron microprobe analyses. (a) Plane polarized light scan as viewed from the bottom of the mount (grain surfaces not exposed on this side). (b) Mount map. Labels refer to sample buckets (numbered 1-4) and bank samples (SB) obtained at the Freeman Mine dump. Sample labels are the same for EMP results. (c) Schematic diagram

prepared in the same manner. However, these grains from the stream gravel were cleaned first with soap and then boiled in oxalic acid for an hour to remove the clay and iron oxide coatings. At least two grams of these samples (**SF2-26-02**, *WF2-26-02*, and NF2-26-02) were also sent to ACME for bulk chemical major element, trace element and REE analysis. Prior to submitting this last batch of cleaned samples for analyses, the minus 80-mesh powder was examined with UVL. It was noted that the **SF** and *WF* powder samples were equally fluorescent and the NF powder sample showed no fluorescence.

Thin-Section Petrography, Fluorescence, Cathodoluminescent, X-Ray and SEM Studies

A polished thin section of 6 zircon crystals was examined using equipment at Virginia Tech and UNC-Asheville. Several opaque inclusions in the zircons were analyzed at UNC-Asheville using an FEI Quanta environmental scanning microscope with an Oxford Inca 450 energy dispersive spectrometer. Thin section photomicrographs were also obtained at UNC-Asheville. The grains in this section (Figure 3a) were also viewed with UVL, using a fluorescence unit attached to a petrography microscope and an Olympus BX-51 luminoscope at Virginia Tech to determine which zircon grains or parts of them were strongly fluorescent and cathodoluminescent. Reddish coatings from several zircon grains were scraped off the crystals and examined at UNC- Asheville by X-Ray Diffraction to determine the mineral(s) content of the coating. SEM-EDS analyses of opaque grains were also done at UNC-Asheville.

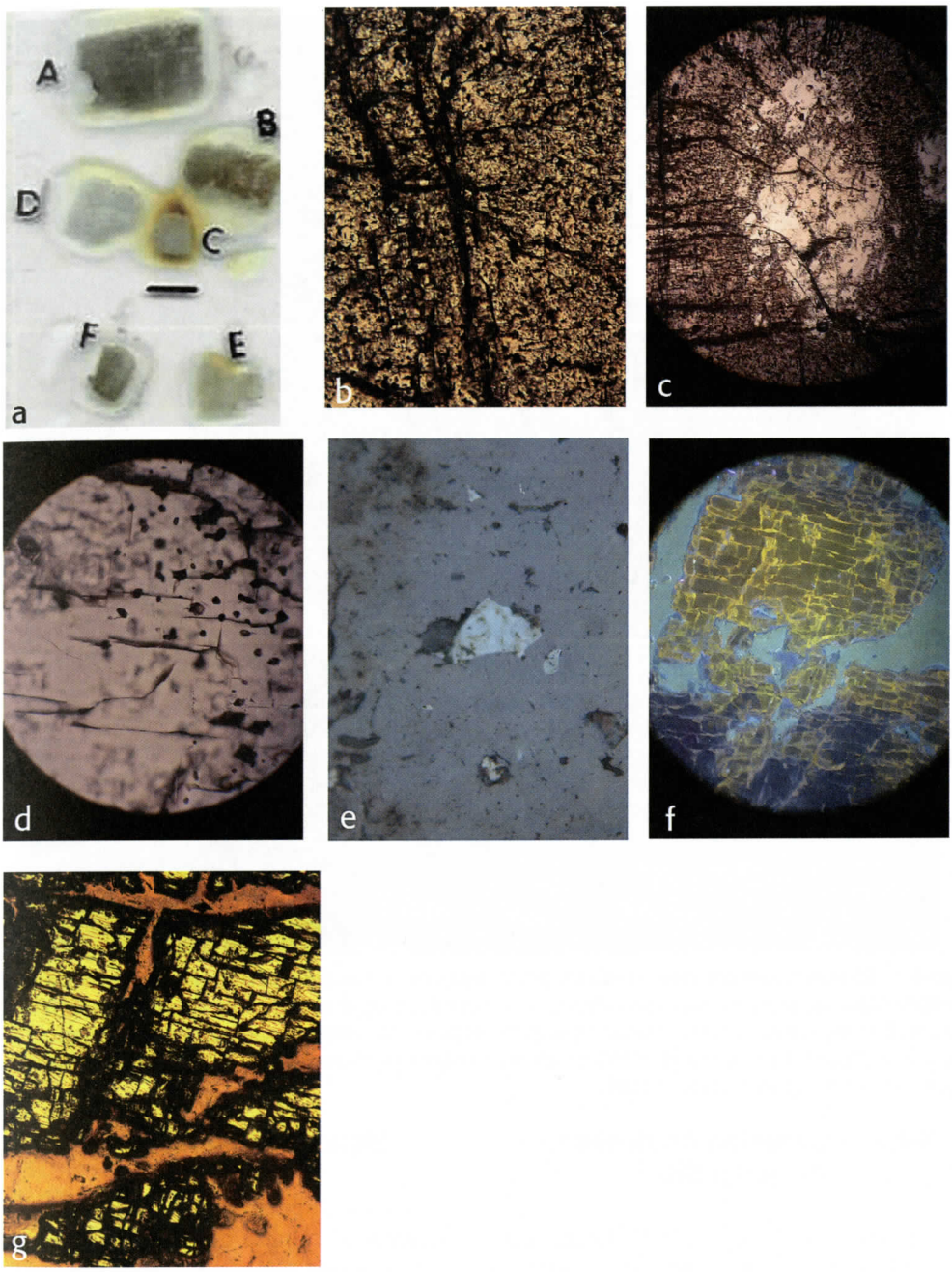

Figure 3.a. Polished thin section of 6 zircon crystals A-E. Bar is 0.6 cm wide; b. Mottled texture in grain A, (field of view (fov is 1.5 mm) Photo courtesy J.W. Miller, UNC- Asheville; c. Mottled texture in grain A, and clear, light football-shaped area, (first generation of crystallization?), (fov =2mm). Photo courtesy of R. J. Bodnar, Virginia Tech; d. Melt inclusions in grain D (fov= 0.4mm), Photo courtesy of R. J. Bodnar; e. Magnetite grains (light areas) in grain B in reflected light (fov= 0.3mm), Photo courtesy of J.W. Miller; f. Fluorescence along fractures in grain D (light areas), (fov= 2mm) photo courtesy of R. J. Bodnar; 4g. Strongly cathodoluminescence zones (light areas) in grain D, (fov= 4mm), photo courtesy R. J. Bodnar.

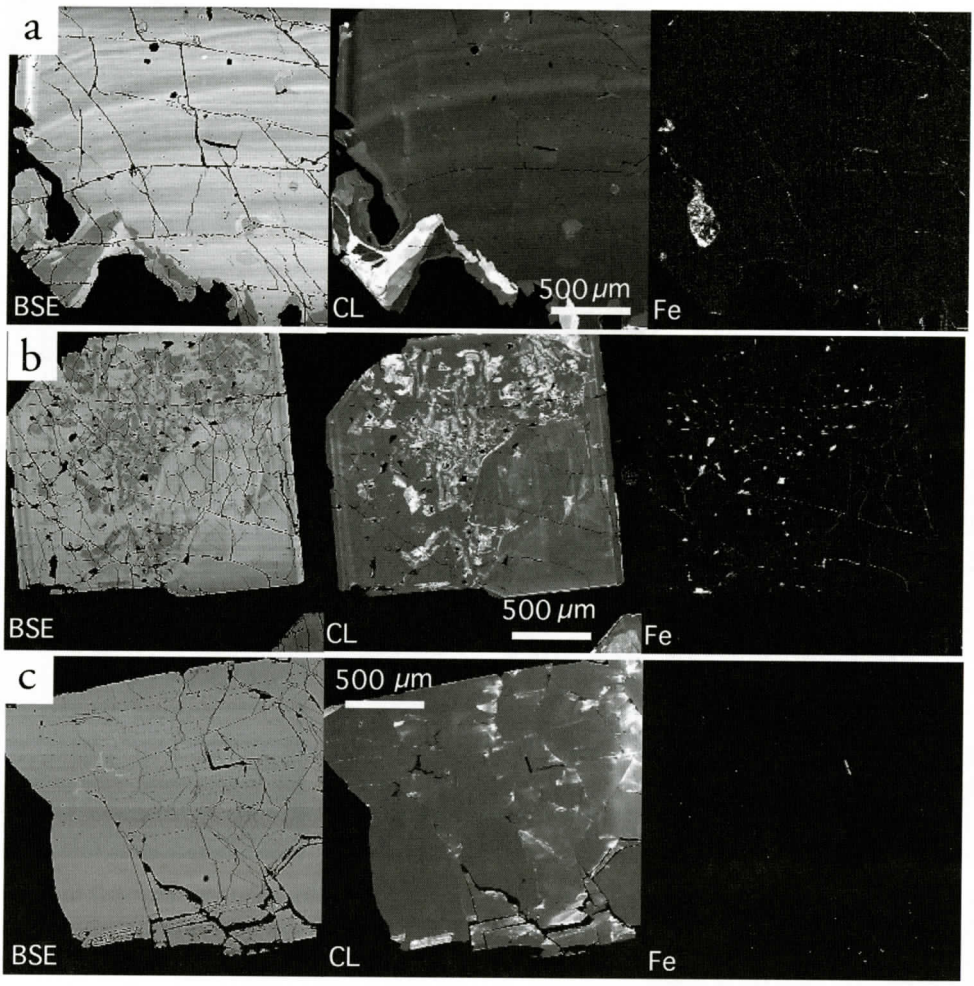

Figure 4. Zircon backscattered electron (BSE) images, cathodoluminescence (CL), and Fe elemental maps for selected samples shown in Figure 2. Images at the same scale and scale bar of 0.5 cm (500 m) is the same for the sample suite shown. For reference all grains are shown in Figure 2 and Figure 4a is sample #SB-2 (high fluorescence), Figure 4b is # 2-1 (low fluorescence), Figure 4c is #2-2 (low fluorescence).

X-Ray Diffraction Analyses for Metamict State

Samples of both **SF** and *WF* zircons were ground in an agate mortar and pestle and mixed with NIST 640c silicon for powder diffraction. Samples were run on Appalachian State University's Kratos XRD 6000 unit from 19°-140° 2θ, with a step size of 0.04 and a count time of 9.6 seconds. Peaks were indexed by analogy to JSPDS-ICDD cards 06-0266, 13-1374, and an independently calculated pattern.

Bulk Chemical Analyses

For each population (**SF**, *WF*, and NF) a minimum of 2 grams of greater than 40-mesh zircons, ground to minus 80-mesh were submitted to ACME for major, trace element, and REE analyses. After preparation by $LiBO_2$ fusion of 0.2 grams of zircon, major elements were analyzed by inductively coupled plasma optical emission spectroscopy (ICP-OES). Inductively coupled plasma mass spectrometry (ICP-MS) at ACME was also used to determine trace

elements and minor elements, including rare earth elements: La, Ce, Pr, Nd, Sm, Eu, Gd, Tb, Dy, Ho, Er, Tm, Yb, and Lu, after $LiBO_2$ fusion of 0.2 grams of zircons.

Electron Microprobe Analyses

Eight *WF* and seven **SF** ~0.5 cm zircon grains were obtained from the weathered dump samples for electron microprobe (EMP) analysis (Figure 2). These grains were mounted in epoxy and polished to the outermost level for imaging and quantitative analyses (Figure 2c). Only backscatter (BSE) and cathodoluminescence (CL) images were obtained at the second polish level. Qualitative and quantitative chemical data across portions of **SF** and *WF* grains were collected with a Cameca SX-52 EMP at the University of Tennessee. Backscattered electron (BSE) and cathodoluminescence (CL) images (Figure 4) were obtained while mapping qualitative elemental abundance for Zr (La_α PET), Fe (K_αLIF), Th (M_αPET), Y (L_αTAP), and U (M_αPET) over the same area at the first polish level. Well-characterized natural and synthetic standards (zircon for Zr; baddelyite for Hf; ThO_2 for Th; hematite for Fe, and U for U) prepared by the C.M. Taylor Corporation were used to calibrate the instrument prior to quantitative analyses and a ZAF correction procedure was applied. An acceleration voltage of 20 kV and beam current of 30nA were used, with a 2μm beam size for quantitative traverses consisting of 10-20 spots per traverse, with an average of 1 analysis per ~10 μm. Quantitative analyses were also obtained on several very bright (in BSE) inclusions. Major component oxide weight percents were also obtained for SiO_2 and ZrO_2. The following trace element oxides were also included in the analytical routine: U_2O_3, HO_2, ThO_2, Al_2O_3, Fe_2O_3, Y_2O_3, MgO, and CaO; however, only HfO_2 and U_2O_3 were consistently at or above detectable concentrations.

RESULTS AND DISCUSSION

Nine weathered pegmatite hand samples contain 1% zircon by weight from the greater than 40-mesh fraction. *WF* zircons from these weathered bank samples were 12x more abundant than the **SF** zircons. One weathered pegmatite sample weighed 750 grams and yielded 20.3 grams of plus 40-mesh zircons. Weight percent zircons in the nine weathered samples ranged from 0.13% – 2.7%. **SF** zircons tend to be pink-gray in color, whereas the *WF* and NF zircons tend to be dark, (pale orange-brown), and have more pronounced iron oxide staining on their surfaces. X-ray diffraction analysis confirmed this stain to be mainly goethite with minor hematite (personal communication, J.W. Miller, 2006). Other minerals noted in the coarse, heavy panned concentrates included magnetite, garnet, tremolite (?), epidote and limonite pseudomorphs after pyrite.

Petrographic studies in transmitted light also indicated that the darker, *WF* grains are mottled (Figure 3a, grains A, B, C, F) but that portions of the grains contain clear areas (Figure 3c). Figure 3a is of poor quality but it illustrates the color differences between the grains and this slide was unfortunately destroyed before another photograph could be taken. The brown orange mottling (Figure 3b) appears to be caused by very small inclusions (<0.05mm). Numerous clear, colorless mineral(s) occur in the zircons and were too small (0.05 mm) to be identified. Small fluid inclusions (<0.01mm) were also found in the grains (Figure 3d) (personal communication, Dr. Robert Bodnar, 2006). All crystals A-F (Figure 3a) examined under reflected light contain small inclusions (<0.1mm) of an opaque mineral (Figure 3e). Several grains of this opaque mineral were analyzed by SEM-EDS at UNC-Asheville. The weight percent of Fe in these opaques varied from 72.4% – 76.9%, (personal communication, J.W. Miller, 2006), identifying this opaque as magnetite. A reflected light study confirmed that the opaque grains are magnetite. Areas of higher Fe observed in some of the EMP-Fe elemental maps (Figure 4b), may represent the location of magnetite grains, and weathered magnetite grains in the pits, as well as the goethite/hematite in fractures or cavities (Figures 4a; b). How-

Table 1. Bulk chemical analyses of zircon crystals from the Freeman Mine dump and stream.

Sample Number	Weight % Fe_2O_3	Weight % TiO_2	Weight % P_2O_5	Weight % ZrO_2	ppm U	ppm Th	ppm Hf	ppm Y	ppm Dy	ppm REE + Y
SF12-13-00	2.09	0.08*	0.05*	56.87	1441	3176	10371	250*	NA	NA
WF12-13-00	3.83	0.08*	0.05*	56.01	1638	3146	10907	284*	NA	NA
SF11-22-01										
SF-1	1.76	0.1	<0.01	68.6	1309	1569	8830	1402	148	2896
SF-2	1.58	0.17	0.01	69.07	1015	1788	7888	1174	135	2210
SF-3	0.94	0.13	<0.01	71.05	219	778	6126	779	102	2149
SF-4	0.74	0.04	0.09	71.04	598	3305	7497	1788	243	5750
4 samples										
Range	0.74 - 1.76	0.04 - 0.17	<0.01 - 0.09	68.60 - 71.05	219 - 1309	778 - 3305	6126 - 8829	779 -1788	102 - 243	2149 - 5750
Average	1.26	0.11	0.03	69.98	785	1860	7585	1286	157	3251
WF11-22-01										
WF-1	12.17	0.37	0.2	54.1	1567	2029	8332	1660	174	3665
WF-2	3.96	1.88	0.39	55.73	1874	2729	8805	1817	225	4260
WF-3	1.65	1.37	0.03	67.85	870	2556	7085	1482	188	2851
WF-4	2.13	1.04	0.12	62.03	965	3024	8051	1662	228	6179
4 samples										
Range	1.65 - 12.17	0.37 - 1.88	0.03 - 0.39	54.10 - 67.85	870 -1874	2029 - 3024	7085 - 8804	1660 -1817	174 - 228	2851 - 6179
Average	4.98	1.17	0.19	59.92	1319	2585	8068	1655	204	4239
Cleaned samples										
SF2-26-02	0.86	0.02	0.04	63.38	676	3694	5423	1491	232	2911
WF2-26-02	0.71	0.01	0.02	62.89	868	3194	5645	1439	214	2793
NF2-26-02	1.09	0.02	0.09	60.86	2164	4003	7801	3174	434	5857

SF-Strong Fluorescence, WF- Weak Fluorescence, NF- No Fluorescence, NA-No Analyses * denotes plups of original samples run later

ever, not all of the Fe-elemental maps showed the presence of Fe-rich areas (Figure 4c).

A limited petrographic paragenetic study of the zircons indicates at least three periods of zircon crystallization: an initial clear phase, a darker mottled phase (Figure 3c), and a final clear phase. This final clear phase that filled fractures and portions of rims of some of the grains is indicated by some highly fluorescent portions of grains such as exhibited in Figure 3f.

Two clear crystals (D and E, Figure 3a) show strong fluorescence (Figure 3f, crystal **D** in Figure 3a), whereas dark, red-brown crystals (A, B, and F in Figure 3a) display few areas of strong fluorescence. Darker zircon grains (A, B and F in Figure 3a) examined under plain light are heavily mottled (Figure 3b, grain A in Figure 3a) and appear red-brown. In general, the fluorescent/cathodoluminescence zones in these red-brown crystals are confined to small areas, fracture fillings and grain edges. Luminoscopic results were similar to the UVL fluorescent results in that the only grains demonstrating strong CL (Figure 3g) were those that did not have a dark red-brown color (i.e., zircons D; E in Figure 3a). Strong CL in the dark, mottled grains (zircons A,B; F in Figure 3a) was generally confined to the clear portions on rims, patches, or fractures.

Zoning of Freeman Mine zircons varies from relatively simple oscillatory patterns (Figure 4a) to complex "patchwork" textures of bright and dim CL regions (Figures 4b; c) similar to those presented by Hoskin and Schaltegger (2003) and by Corfu et al. (2003). Areas that are darker in BSE (Figure 4) indicate elements with atomic numbers lower than Zr and in general exhibit greater cathodoluminescence.

Bulk chemical analyses of the first batch (*WF12 -13-00*; **SF12-13- 00**) of zircon grains, from dump material indicate *WF* zircons have slightly higher concentrations of U (14% greater equal to ~ 200 ppm), Hf (5% greater equal to ~500 ppm), much greater Fe_2O_3 (83% greater equal to ~1.75%), relative to **SF** zircons (Table 1). Higher Fe values in the *WF* zircons may, in part, be attributed to magnetite inclusions and iron oxide coatings along the surface of the grains, fractures and cavities. Average values for bulk chemical analyses of the second set of grains, from dump and stream gravels, which includes 4 sets of *WF* fluorescent zircons and 4 sets of **SF** zircons (Table 1, *WF 11-22-01*; **SF 11-22-01**), have higher average levels of Fe_2O_3 (5% vs. 1.3%), TiO_2 (1.17% vs. 0.11%), P_2O_5

Table 2. Minimum, maximum, and mean electron microprobe values for quantitative analytical traverses across zircons at the level of the first polish.

			SiO_2	ZrO_2	HfO_2	ThO_2 (0.08%)		Fe_2O_3 (0.03%)		U_2O_3 (0.1%)		TOTAL	
	Traverse	N	Mean (1σ)†	Mean (1σ)†	Mean (1σ)†	Mean (1σ)†	n	Mean (1σ)†	n	Mean (1σ)†	n	Mean (1σ)†	n
weakly flourescent	1	10	32.3 (4)	67.1 (7)	1.9 (3)	0.14 (2)	3	0.08 (4)	4	0.29 (19)	10	101.8 (6)	10
	2#	9	32.5 (2)	68.0 (6)	1.6 (2)	--	1	0.22 (30)	3	0.21 (5)	8	102.4 (5)	9
	3	10	32.4 (4)	68.2 (4)	1.3 (1)	--	0	0.1 (1)	2	0.31 (11)	10	102.4 (6)	10
	4	10	31.2 (7)	66.4 (10)	1.7 (4)	0.10 (1)	5	--	0	0.21 (7)	9	99.7 (12)	10
	5	10	31.8 (5)	67.2 (6)	1.7 (3)	0.13 (5)	3	0.12 (4)	2	0.19 (5)	8	101.2 (8)	10
	6	10	32.0 (3)	66.9 (8)	2.0 (3)	--	1	--	0	0.18 (4)	10	101.1 (8)	10
	1-6	59	32.0 (6)	67.3 (9)	1.7 (3)	0.11 (3)	13	0.13 (15)	11	0.23 (11)	55	101.4 (12)	59
strongly fluorescent	7#	9	32.2 (5)	67.0 (11)	2.0 (3)	--	1	--	0	0.12 (1)	4	101.2 (14)	9
	8	15	32.1 (5)	67.3 (11)	1.7 (2)	0.15 (5)	9	0.10 (6)	4	0.20 (8)	14	101.6 (10)	15
	9	11	32.7 (1)	69.5 (6)	0.9 (1)	--	1	--	1	--	1	103.2 (7)	11
	10	9	32.4 (2)	68.9 (14)	0.8 (1)	0.13 (3)	5	--	0	0.11 (2)	2	102.3 (14)	9
	11	10	32.3 (3)	68.4 (10)	1.0 (2)	--	1	--	0	0.14 (2)	3	101.9 (11)	10
	12	20	32.6 (2)	68.8 (7)	1.0 (3)	--	0	--	0	0.12 (1)	4	102.5 (6)	20
	7-12	74	32.4 (4)	68.3 (13)	1.2 (5)	0.13 (5)	17	0.08 (6)	5	0.16 (7)	28	102.2 (11)	74
ALL	1-12	133	32.2 (5)	67.9 (12)	1.4 (5)	0.12 (4)	30	0.12 (13)	16	0.21 (10)	83	101.8 (12)	133

*n = number of analyses above detection limit; detection limit noted next to oxide where n<N.

†One sigma values for last reported digit.

#Analysis removed with low totals (95% in traverse 2 and 92% in traverse 7).

(0.19% vs. 0.03%), U (1319 ppm vs. 785 ppm), Th (2585 ppm vs. 1860), Hf (8068 ppm vs. 7585 ppm), Dy (204 ppm vs.157 ppm), and total REE + Y (4239 ppm vs. 3251 ppm) in the WF zircons than in the SF ones. Average ZrO_2 values are higher for the SF, versus WF sets of un-cleaned zircons, averaging ~70% vs. ~ 60% respectively.

Chemical analyses of the third batch, (**SF2-26-02**; *WF2-26-02*; NF- 2-26-02), of zircons from the stream gravel that were cleaned with soap and oxalic acid were similar to previous analyses (Table 1) except for one *WF2-26-02* sample discussed below. NF zircons have, respectively, higher contents of Fe_2O_3 (1.09 vs. 0.86%), Hf (7801 vs. 5423 ppm), U (2164 vs. 676 ppm), Th (4003 vs. 3694), Dy (434 vs. 232 ppm), and total REE plus Y (5857 vs. 2911 ppm) than the **SF** ones. **SF** zircons have higher ZrO_2 values of 63.4% as compared to 60.9% than NF ones. The cleaned *WF2-26-02* sample yields the lowest Fe_2O_3 values (0.71%) of any bulk chemical analyses (Table 1). Chemical analyses for this sample *WF2-26-02* are more similar to that of the **SF2-26-02** and other SF samples (Table 1). After grinding, the powdered sample *WF-2-26-02* showed no difference in fluorescence from that of the **SF2-26-02** powdered sample and both were fluorescent.

The third batch of samples — the cleaned zircons — confirmed higher Fe_2O_3 levels in the NF zircons (1.09 vs. 0.86%). However one batch of cleaned zircons, labeled as (*WF2-26-02*, Table 1) actually has the lowest Fe_2O_3 values of any samples submitted. These lower Fe_2O_3 results (0.71%) in the *WF2-26-02* batch of zircons might have had *WF* outer zones and a core of **SF** zircon. This is most likely the case since the powder of the *WF* sample showed no difference in fluorescent properties when compared to the **SF** powdered sample. Chemical analyses for this *WF* sample are similar to those of the **SF** samples i.e. higher Zr, lower U, Th, Hf, Y, Dy, and total REE + Y. This may indicate that this *WF* sample had a number of grains with strong fluorescence not noticed by the UVL study when the sample was prepared. Zoning of **SF** and *WF* areas within grains may have also influenced other bulk analyses reported in Table 1. Zoning i.e. high and low fluorescent zones with varying chemistry within grains may also account for variation in differences in bulk chemical analyses of other samples.

The mean EMP analyses for **SF** and *WF* groups overlap within 1α for each oxide component (Table 2). These results are not statistically significant but the EMP results appear to indicate slightly higher percentages of Fe_2O_3, HfO_2, U_2O_3 in the *WF* grains. HfO_2 was the only minor component present in all analyses and the only non-major component with mean values greater than 1% in most traverses. Aver-

age HfO_2 levels were 0.5% higher in the *WF* grains (Table 2). Only 12% of the EMP analyses had Fe_2O_3 above the 0.03% detection limit; however, more than half of the analyses with detectable Fe_2O_3 were from the *WF* grains, with 5 of the 7 > 0.1%. Overall the average Fe_2O_3 values were 0.05% higher in the *WF* grains. U_2O_3 was detected in over 90% of the *WF* samples and in less than 50% of the **SF** samples. *WF* grains exhibited a slightly higher average U_2O_3 value of 0.23%. The **SF** zircons also averaged about 1% more ZrO_2 than the *WF* samples. Traverses across two grains (one **SF** and one *WF*) show decreased CL brightness with increasing HfO_2. Two EMP analyses of a bright inclusion (in BSE) identified a thorium-rich (ThO_2 = 9.5%, 9.8%) and yttrium-rich (Y_2O_3 =19.7%, 27.2%) silicate mineral (yttrialite?) with no P_2O_5. The overall totals for this grain from two analyses are low (76.1%, 69.7%), thus its identity cannot be confirmed. Spandler, et al (2004) noted the presence of yttrialite as inclusions in zircon from northeastern New Caledonia, so it is possible that there might be yttrialite in the Freeman Mine zircons as well.

Disparate bulk chemical and EMP results for minor and trace elements is most certainly due to orders of magnitude differences in terms of volumes analyzed (i.e., bulk chemical analyses represent multiple grains and inclusions). Slightly lower levels of Hf and Zr in bulk chemical analyses versus EMP analyses might also be explained in terms of dilution of pure zircon with inclusions (Table 1). The variability noted in the U and Th ion microprobe (not shown) and EMP data (Table 2) suggests that trace elements are distributed on a small-scale (i.e, tens of microns) within individual grains; however, bulk chemical data also suggests that individual whole grains may be contributing to elevated U, Th, Hf, Y and summed REE+Y concentrations (i.e., NF2-26-02 illustrated in Table 1).

X-ray diffraction powder patterns of several ground **SF** and *WF* zircon samples exhibit little difference in peak positions, shape, or width, indicating virtually no difference in unit cell dimensions between zircon populations. The refined unit cell dimensions for the **SF** sample (α=6.6087[17]Å, c=5.9949[28]Å) and the *WF* sample (a=6.6094 (31Å), c=5.9959 (50Å)) are consistent with only minor metamictization, which also holds for the weakly to non-fluorescent samples when the pattern similarities are taken into account. As noted by Speer (1982), Hf substitution up to 40 mole percent in zircon produces a change of less than 0.01 Å in the a and c cell dimensions. More significant cell dimension changes are due to metamictization, which causes the expansion of α from 6.600 to 6.7505 Å and c from 5.975 Å to 6.090 Å as α activity increases (Speer, 1982). As there is little difference in cell dimensions it appears that metamictization is not the cause of the difference in fluorescence in the populations of zircons at the Freeman Mine.

In addition to the data presented here, Freeman Mine zircon (IMP) U-Pb geochronology was obtained as part of a complimentary study (Bream, 2003). Despite their large size and multiple growth zones, Freeman Mine U-Pb zircon ages are remarkably consistent and statistically indistinguishable from **SF** (327 ± 3 Ma, n = 5/5, MSWD = 2.17) and *WF* (326 ± 3 Ma, n = 4/6, MSWD = 1.02) grains (Bream, 2003). Ion microprobe U-Pb ages for **SF** and *WF* zircons yield ages that are within 2σ error of one another, suggesting that the distinct fluorescent populations crystallized during the same event or within a ~7 m.y. window. Furthermore, IMP analytical spots display a wide range of U and Th concentrations within individual **SF** and *WF* grains from < 50 to >2100 ppm U and from <60 to >4900 ppm Th, with Th/U ratios from 0.02 to approximately 7 (Bream, 2003). Of interest is that the highest IMP U concentration observed (Bream, 2003) was from a *WF* grain (2182 ppm).

Gaft et al (2005) suggest that for any mineral to be luminescent (in this case fluorescence and cathodoluminescence) that three conditions must be met. These conditions are (1) a crystal lattice suitable for forming emission centers, (2) a significant number of these luminescent centers, and (3) few quenchers. In the case of zircon, Gaft et al (2005) note that these luminescent centers are caused by Dy^{3+} and Eu^{3+}. Other REE, particularly Dy are also noted

as a possible cause of CL (e.g., Mariano, 1989; Remond et al, 1992). In their studies of detrital zircons, Van Es et al (2000) also noted that Dy and Tb are the important activators for luminescence. Nasdala et al (2003) state "that CL is not only determined by the chemical composition of the sample but is strongly controlled by the structural parameters such as crystallinity or the presence of defect centers". Cathodoluminescence in zircon has also been related to any of the transition elements (Klein and Hurlbut, 1999).

In addition Gaft et al (2005), note that the yellow fluorescence in zircon decreases rapidly when specimens are heated above 700° C and disappears entirely upon reaching 800° C. Gaft et al. (2005) also concluded that the luminescence in this instance was derived from color centers created by the decay of radioactive constituents such as U and Th. Older references suggest that fluorescence activation in zircon by shortwave UVL is usually attributed to elevated concentrations of trace elements, including U, which was identified as the cause of the brilliant yellow fluorescence in Australian zircons (Mumme, 1967). Hf was reported as a possible cause of this fluorescence in the Zirconia District (Warren, 1944). Drake (1953) also noted that Henderson County, North Carolina, zircons are orange-brown in color, fluoresce vivid yellow; thus they suggested that the cause of fluorescence was due to excess Hf.

Our limited bulk chemical analyses (Table 1) showed that *WF* Freeman Mine zircons generally have higher Fe_2O_3, U, Hf, Th, Dy and total REE plus Y and lower ZrO_2. EMP data (Table 2) also show that the *WF* grains are generally higher in HfO_2, U_2O_3 and Fe_2O_3 even though there is overlap at the 1 sigma level. Average ZrO_2 is higher in the SF grains. Fe_2O_3 levels in bulk chemical analyses are higher in *WF* uncleaned zircons, averaging 2.5x greater than SF (Table 1). Sample *WF-1*, with a value of 12.17% Fe_2O_3, skews the average results (Table 1). However, in each of the other three instances the Fe_2O_3 values for the *WF 11-22- 2-4* batches of zircons are higher than those of the **SF** analyses. The third batch of samples — the cleaned zircons — confirmed higher Fe_2O_3 levels in the NF zircons (1.09 vs. 0.86).

Based solely on the majority of these limited bulk chemical analyses, the EMP data and the presence of magnetite inclusions, and Fe as coatings in other areas, it is possible that increased Fe may have quenched luminescence — a decrease in the intensity of fluorescence and luminescence — in zircons at the Freeman Mine. Baker (1962) noted that Fe was believed to be a quencher of fluorescence, and Marshall (1988) stated that, "Ferrous iron is a well known quencher for luminescence in many phosphors." Marshall (1988) also indicates that, in the case of carbonates, Fe as ferruginous stains on the surface and in cracks has no bearing on the luminescence in carbonates; and further to act as a quencher, Fe must be incorporated in the lattice, and perhaps this is possible in the case of the Zirconia zircons. However, Marshall (1988) does indicate that some CL emissions may be absorbed by ferruginous material. This quenching effect was also noted by Waychunas (1988) who implicated that Fe^{3+} as a "killer or poison" for luminescence. Habermann (2003) also noted that Fe^{+2} "can quench CL efficiency" and that the lack of CL could be used as an indicator of high Fe. Gaft et al (2005) indicate that concentration quenching by Fe^{3+} is possible. Although there is no indication that Fe fits into the zircon structure in this present study, Gaft et al. (2005) indicate that transition metals such as Cr^{+3}, Mn^{+2} do fit into the zircon structure and note that Fe^{+2} is an intrinsic quenching metal. Because of this information and our data, we are unwilling to exclude the possibility that some of the Fe in our analyses is in the structure of the zircon itself and that iron may actually be contributing to the quenching.

Another cause for the decreased fluorescence in the case of the Freeman Mine zircons may be excessive REE + Y, as indicated by the bulk chemical analyses or higher U. Excessive REE levels have also been noted as a quenching agent (Speer, 1982) and may be the cause of weak to non-fluorescence in some zircons from the Freeman Mine.

Freeman Mine zircons provide an opportunity to correlate shortwave UVL fluorescence

with a number of variables, including bulk chemistry, petrographic features, crystal structure, detailed μm-scale EMP, IMP analyses, and age. Results vary in terms of types of chemical analyses, the way the data were reported, some in oxides and some as elemental data, sample scale, and precision. However, this analytical suite allows for interpretation at different scales so that they yield a more complete understanding of these megacrystic zircons.

Based on our data, the weak fluorescence/ cathodoluminescence in zircons from the Freeman Mine could be the result of any or all of the following: (1) Fe in inclusions, particularly magnetite, (2) Fe in the zircon crystal structure, (3) Fe coatings on the *WF* and NF grains (4) excessive REE concentrations, and/or (5) higher U and/ or Hf masking the fluorescence.

CONCLUSIONS

- Limited bulk chemical analyses of *WF* Freeman Mine zircon grains have higher concentrations of Fe, U, and/or total REE plus Y, and possibly Hf. Higher average U is also noted in the *WF* zircons in the electron microprobe analyses. This apparent relationship is unusual when compared to the literature which states that these elements, U, Hf, and REE, are cited as the *cause* of fluorescence. Therefore, we propose that Fe and total REE + Y are possible causes for the quenching of the fluorescence and the cathodoluminescence.
- Magnetite is an opaque mineral found in both **SF** and *WF* grains. Yttrialite may also be present as very small inclusions in the zircons.
- Cell dimensions determined by X-ray diffraction for **SF** and *WF* zircons show no differences suggesting only minor metamictization.
- Results of this study may have economic benefits for heavy mineral companies preparing zircon concentrates. Based on limited analyses in this study, higher fluorescence corresponds to higher Zr and lower Fe values. If higher total REE content plus Y and Fe is desired, then weakly to non-fluorescent zircon grains should be concentrated.

ACKNOWLEDGEMENTS

We would like to thank Appalachian State University's Graduate School for funding some bulk chemical analyses. We would also like to thank Vulcan Materials Company for funding the Vulcan Materials Company's Economic Geology Laboratory at Appalachian State University where much of the work was completed and for their support of our programs. The authors would like to thank the Stepp and Rydberg families, for allowing us access to their properties to collect the zircons. Callahan would like to thank Dr. R. J. Bodnar and his two graduate students, Steve Becker and Mathew Severs, as well as Charles Farley at Virginia Tech for their help in taking fluorescent, petrographic and cathodoluminescent pictures of the crystals. He would also like to thank Dr. J. William Miller at UNC-Asheville for the SEM magnetite analyses and reflected and transmitted light pictures of zircon crystals. The authors would like to also thank Dr. Melissa E. Barth of Appalachian State University for her editorial comments. Bream wishes to thank Allan Patchen for use and assistance with the University of Tennessee electron microprobe facility. Bream was supported during this research by National Science Foundation grant EAR-9814800 (PI's: R.D. Hatcher, Jr. and C.F. Miller) and the University of Tennessee Science Alliance Center of Excellence. The authors would especially like to thank Dr. William Ranson of Furman University and Dr. Kelly Vance of Georgia State University for their review and constructive comments of an earlier version of the manuscript.

REFERENCES

Baker, G., 1962, Detrital Heavy Minerals in Natural Accumulates: Australian Institute of Mining and Metallurgy, Monograph Series n.1, p.73.

Bream, B.R., 2002, The southern Appalachian Inner Piedmont: New perspectives based on recent detailed geologic mapping, Nd isotopic evidence, and zircon

geochronology, *in* Hatcher, R.D., Jr., and Bream, B.R., eds., Inner Piedmont geology in the South Mountains-Blue Ridge Foothills and southwestern Brushy Mountains, central-western North Carolina: North Carolina Geological Survey, Carolina Geological Society annual field trip guidebook, p. 45-63.

Bream, B.R., 2003, Tectonic implications of para-and orthogneiss geochronology and geochemistry from the southern Appalachian crystalline core [Ph.D. dissertation]: Knoxville, University of Tennessee, 296 p.

Corfu, F., Hancher, J.M., Hoskin, P.W.O., and Kinny, P, 2003, Atlas of zircon textures, In Zircon, Reviews in Mineralogy and Geochemistry, J.M, Hancher and P.W.O. Hoskin, eds., Mineralogical Society of America, Bulletin v. 53, p. 469-500.

Davis, T.L., 1993, Lithostratigraphy, structure, and metamorphism of a crystalline thrust terrane, western Inner Piedmont, North Carolina [Ph.D. dissertation]: Knoxville, University of Tennessee, 245 p.

Drake, H.C., 1953, The uranium and fluorescent minerals, Mineralogist Publishing Co., 79 p.

Gaft, M., Reisfeld, R. and Panczer, G. 2005, Luminescense Spectroscopy of Minerals and Materials, Springer-Verlag, Berlin, 356 p.

Habermann, A., 2003, Quantitative cathodoluminescence (CL) spectroscopy of minerals: possibilities and limitations, Mineralogy and Petrology, v. 76, p. 247-260.

Hoskin, Paul, W.O. and Schaltegger, Urs., 2003, The composition of zircon and igneous and metamorphic petrogenesis:, In Zircon, Reviews in Mineralogy and Geochemistry, J.M, Hancher and P.W.O. Hoskin, eds., Mineralogical Society of America, Bulletin v. 53, p.27-62.

Klein, C. and Hurlbut, S., Jr., 1999, Manual of Mineralogy after James D. Dana, John Wiley and Sons, Inc. New York, 681p.

Mariano, A.N., 1989, Cathodoluminescence emission spectra of rare earth element activators in minerals, *in* Lipin, B.R., and McKay, eds., Geochemistry and mineralogy of rare earth elements, American Mineralogical Society Reviews in Mineralogy, v. 21, p. 339-348.

Marshall, D. J., 1988, Cathodoluminescence of geological materials, Unwin Hyman, Boston, p. 146.

Mumme, I.A., 1967, On the radioactivity and related fluorescent properties of sedimentary Australian zircons: Transactions Royal Society Australia, v. 91, p. 27-29.

Nasdala, L., Zhang, M., Kempe, U, Panczer, G., Gaft, M., Adrut, M and Plštze, M, 2003, Spectroscopic methods applied to zircon. In Zircon, Reviews in Mineralogy and Geochemistry, J.M Hancher and P.W.O. Hoskin, eds., MSA Bulletin v. 53 p. 469-500.

Olson, J., 1952, Pegmatites of the Cashiers and Zirconia districts, North Carolina: North Carolina Department of Conservation and Development Bulletin, n. 34, p. 32.

Ranson, W.A., Williams, I.S., and Garihan, J.M., 1999, SHRIMP zircon U-Pb ages of granitoids from the Inner Piedmont of South Carolina: Evidence for Ordovician magmatism involving Mid to Late Proterozoic crust: Geological Society of America Abstracts with Programs, v. 31, p. 167.

Remond, G., Cesbron, F., Chapoulie, R., Ohnenstetter, D., Roques-Carmes, C., and Schvoerer, M., 1992, Cathodoluminescence applied to the microcharacterization of mineral materials: A Present status in experimentation and interpretation: Scanning Microscopy, v. 6, p. 23-68.

Spandler, C., Herman, J., Rubalto,D., 2004, Exsolution of thortveitite, yttrialite, and xenotime during low – temperature recrystallization of zircon from New Caledonia, and their significance for trace element composition in zircon: American Mineralogist, v.89, p.1795-1806.

Speer, J.A., 1982, Zircon in orthosilicates (Ribbe, Ph.D., Ed.) Mineralogical Society of America, reviews in mineralogy, v. 5, p. 67-112.

Van Es, H.J., Hartog, H.W., de Meijer, R.J., Venema, L.B., Donoghue, J.F. and Rozendaal, A., 2000, Radiation Measurements, v.32, p. 819-823.

Vinson, S., 1999, Ion probe geochronology of granitoid gneisses of the Inner Piedmont, North Carolina and South Carolina [M.S. thesis]: Nashville, Tennessee, Vanderbilt University, 84 p.

Warren, T.S., 1944, List of Fluorescent Minerals: The Mines Magazine, p. 342-343, 363.

Waychunas, G.A., 1988, Luminescence, X-ray emission, and new spectroscopic, in spectroscopic methods in mineralogy, and geology (Hawthorne, F. C., Ed.), Mineralogical Society of America, Reviews in Mineralogy, v. 18, p. 640-698.

SOUTHEASTERN GEOLOGY
V. 45, No.1, June 2007, p. 15-24

AGE OF THE OCMULGEE LIMESTONE (GEORGIA COASTAL PLAIN) BASED ON REVISED METHODOLOGY FOR THE K-AR AGE OF GLAUCONY

ELIZABETH C. STEPHENS[1]

Department of Geosciences, Georgia State University, P.O. Box 4105, Atlanta, GA 30302

JOHN R. ANDERSON, JR.

Science Department, 2101 Womack Road, Georgia Perimeter College, Dunwoody, GA 30338-4497

CHERYL GULLET-YOUNG

Department of Geosciences, Georgia State University, P.O. Box 4105, Atlanta, GA 30302

J. MARION WAMPLER

School of Earth and Atmospheric Sciences, Georgia Institute of Technology, Atlanta, GA 30332-0340

W. CRAWFORD ELLIOTT

Department of Geosciences, Georgia State University, P.O. Box 4105, Atlanta, GA 30302

1. Present address: Department of Earth Sciences, University of Memphis, Memphis TN 38152-3550

ABSTRACT

Grains (0.15-1.0 mm) composed mostly of well-evolved glauconite, based on X-ray diffraction, visual data, and potassium measurement, are found dispersed within the Ocmulgee Limestone (latest Eocene) 20-22 feet above the basal contact at Taylor's Bluff, its type locality, on the Georgia Coastal Plain. These grains are botryoidal and dark grey-green to green-black in color. Some were separated from the limestone for K-Ar age study and yielded an age of 33.7 ± 1.0 Ma from a small sample, 18 mg, used for both potassium and argon-isotope measurements. This K-Ar age for the glauconite places the deposition of this interval of the Ocmulgee Limestone and its characteristic Eocene fossil assemblage close to the time of the Eocene-Oligocene transition (33.9 ± 0.1 Ma). The techniques described herein make it possible to measure the K-Ar age of glauconite present in small amounts using one weigh-out and thus decreasing analytical error. This technique makes it possible to determine numerical age values for limestone containing only small amounts of dispersed but well-evolved glaucony grains.

INTRODUCTION

The terms "glauconite" and "glaucony" are often used interchangeably to refer to a facies composed of green spheroidal pellets and green amorphous clays (Odin and Matter, 1981). Glauconite refers to an iron-rich dioctahedral mica whose tetrahedral sites may contain more than 0.2 trivalent cations (Al or Fe) per formula unit and whose octahedral sites contain 1.2 trivalent cations per formula unit (Bailey and others, 1979). Herein, we refer to the facies and grains as glaucony while reserving the term glauconite for the authigenic phyllosilicate mineral within glaucony pellets.

Glaucony pellets form at the sediment-water interface at depths typically between 50 and 500 meters water depth (Odin and Matter, 1981; Bornhold and Giresse, 1985; Harris and Whiting, 2000). Where slow sedimentation provides a favorable environment, glaucony pellets grow in size and change in both mineralogy and chemical composition from a glauconite-smectite to a glauconitic illite with high (6-8 wt%) potassium (K_2O) content (Bailey and others,

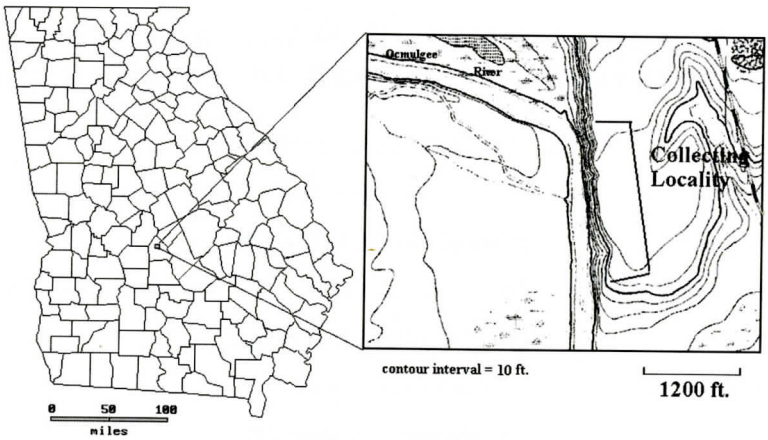

Figure 1: Locality map for Taylor's Bluff, east of the Ocmulgee River, north of Hawkinsville, Georgia., Hawkinsville, 7½ minute Quadrangle.

1979; Odin and Matter, 1981). Odin and Matter (1981) recognized four stages of evolution of the glaucony pellets (nascent, little-evolved, evolved, and highly evolved stages). In this evolution, both potassium and iron contents increase and the glaucony grains change from powdery or crumbly aggregates to larger grains with botryoidal shapes and smooth surfaces. Most of the constituents needed to form glauconite come from the glaucony facies or grains themselves (Odin and Matter, 1981).

During the development and early use of the K-Ar method, glauconite was considered a promising phase for determination of absolute geologic time given the authigenic growth of potassic phases within the glaucony pellets (e.g., Wasserburg and others, 1956; Lipson, 1958; Evernden and others, 1961; Odin, 1982a). Early K-Ar and Rb-Sr age values were typically about 5% less than the values expected from the biostratigraphic positions of the host rocks, which was then thought to be a consequence of diffusional loss of radiogenic Ar (Lipson, 1958; Hurley and others, 1960). Lipson (1958) noted a positive relationship between potassium content and "retention" of radiogenic argon. In some cases, K-Ar age values for glaucony have been larger than the expected values, which may be due to the presence of "inherited argon" within potassic detrital clays in "less evolved" glaucony (Lipson, 1958; Odin, 1982a). "Highly evolved" (6-8 wt.% K_2O) glaucony pellets are found more useful than "less evolved" glaucony pellets (< 4 wt.% K_2O) for determining numerical ages of strata by virtue of being less susceptible to losing radiogenic argon and having less inherited argon (Odin and Velde, 1975; Odin and others, 1977; Odin and Matter, 1981; Odin, 1982a; Odin, 1982b). Age values less than those expected from stratigraphic position may result from argon loss due to increase in temperature after burial to significant depths or from addition of potassium (Thompson and Hower, 1973). Where sediments have not been buried deeply, as for example in the Atlantic Coastal Plain, "evolved" glauconite has been shown to be an excellent K-Ar and Rb-Sr clock for determining the numerical ages of sedimentary strata (Harris and Bottino, 1974; Harris and Fullagar, 1989).

In this study, we describe a method for determination of the K-Ar age of glaucony whereby one weighed sample is used for both potassium and argon-isotope measurements. The K-Ar age of 33.7 ± 1.0 Ma for well-evolved glaucony grains from the Ocmulgee Limestone at its type locality on the Georgia Coastal Plain indicates that the limestone was deposited near the time of the Eocene-Oligocene transition, in the context of the currently accepted time scale for the Paleogene Period (Luterbacher and others, 2004).

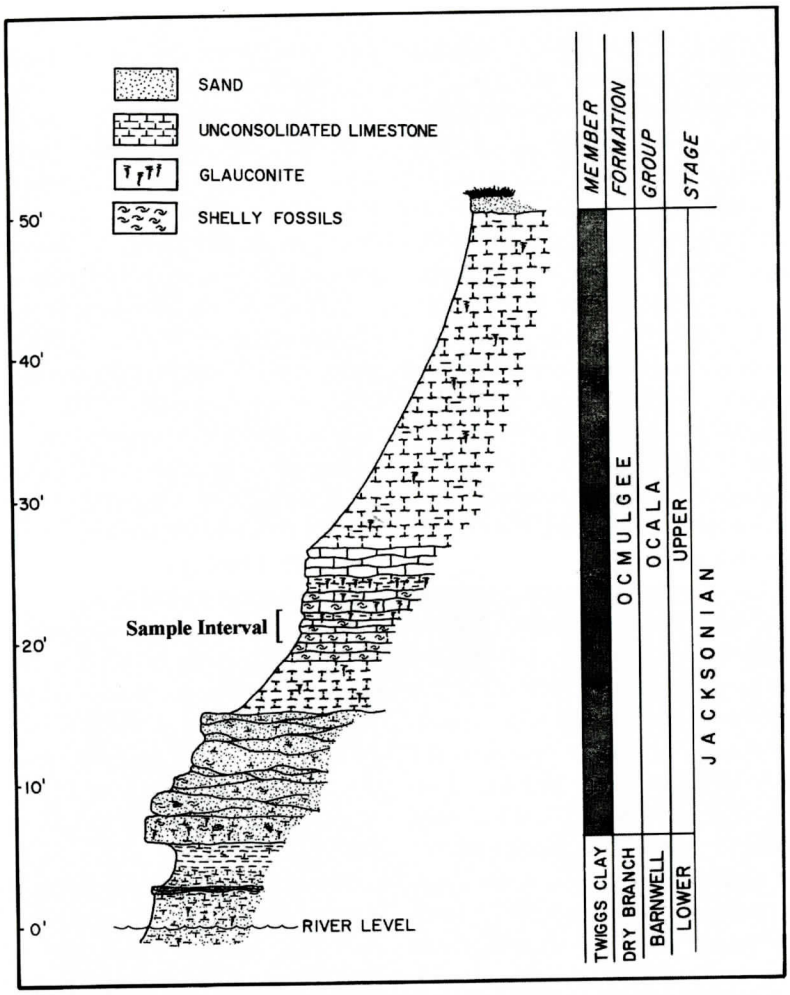

Figure 2: Stratigraphic column of the Ocmulgee Limestone at the type locality at Taylor's Bluff modified from Huddlestun and Hetrick (1986) to show the location of glaucony samples.

GEOLOGICAL SETTING AND LITHOLOGY

The Ocmulgee Limestone, as defined by Huddlestun and Hetrick (1986), extends from exposures in Houston and Pulaski counties eastward at least to the Savannah River. Its character in the east is known from exposures in northern Jenkins County and from Screven County drill cores. Its southern extent is poorly known. The type locality of the Ocmulgee Limestone is at Taylor's Bluff, three miles north of Hawkinsville in Pulaski County (Figure 1). The Ocmulgee Limestone's lithology varies with depth (Figure 2). In some places the limestone near the upper surface of the formation is more argillaceous and much softer than that of the lower section, possibly because of weathering or because that part of the limestone was never well consolidated. The lower section of the limestone is more compact and contains a higher abundance of sand-sized grains and glaucony grains (Huddlestun and Hetrick, 1986).

The Ocmulgee Limestone is highly fossiliferous. The presence of *Chlamys cocoana* (a scallop), was used by Pickering (1970) to suggest an Early Oligocene age for the formation. He noted that *Flabellum cuniformae* (a coral) is found at all outcrops of the formation that are

rather pure calcarenite. Although *F. cuniformae* had been often cited as a Late Eocene guide fossil, Pickering wrote that it occurs throughout the Upper Eocene-Lower Oligocene of the Coastal Plain wherever clean calcarenite occurs. Huddlestun and Hetrick (1986) indicated that *Chlamys cocoana* is no longer thought to be restricted to early Oligocene and placed the Ocmulgee Formation in the uppermost part (upper Jacksonian Stage) of the Eocene epoch. Bryozoans are found throughout the formation. Among these *Ochetosella jacksonica* was used to place the Ocmulgee Limestone in the Late Eocene epoch (Canu and Bassler, 1920; Wortman and others, 2004). The echinoids *Periarchus quinquefarius*, *Paraster americanus,* and *Brissopsis blanpiedi* and the foraminifer *Globigerina sp.* are also present.

In Pulaski County, the Ocmulgee Limestone is overlain by the Marianna Limestone of the Vicksburg Group and is underlain by the Twiggs Clay Member of the late Eocene Dry Branch Formation (Huddlestun and Hetrick, 1986; Huddlestun, 1993). To the east, the Eocene Sandersville Limestone Member of the upper Eocene Tobacco Road Sand has been correlated to the Ocmulgee Limestone based on the presence of the echinoid *Periarchus quinquefarius* in both units (Pickering, 1970; Huddlestun and Hetrick, 1986; Suurmeyer and others, 2003).

METHODS

The original sample was collected at the type locality from an interval 20-22 feet above the base of the limestone (*i.e.*, above the Twigg's Clay) in 2003 (Figure 2). Glaucony grains were separated magnetically from the insoluble residues (primarily quartz) produced by reacting the limestone with 10% hydrochloric acid. The sample was further purified by hand-sorting under a stereomicroscope (40× magnification) using a paintbrush dampened with de-ionized water. Dark grayish green and greenish black botryoidal grains that ranged in size from 0.15 mm to 1.0 mm were picked for analysis in this study. The selected grains were washed on a 0.15 mm sieve to remove contaminants too small to maneuver with a paintbrush or probe.

A small amount of the glaucony grains (~20 mg) was powdered in an agate mortar and pestle. An oriented mount of the powdered sample was scanned in a Philips Norelco X-ray diffractometer equipped with a Bragg-Brentano geometry diffractometer and the MDI Databox to run the scans and plot the diffraction data. The sample was solvated in ethylene glycol vapor for 24 hours and re-scanned to determine the presence of expandable minerals. The X-ray diffraction patterns were interpreted from diffraction data of Moore and Reynolds (1997). Throughout the course of this work, representative glaucony grains were set aside to be examined with a LEO 1450 scanning electron microscope (SEM) at the Georgia State University's Department of Biology.

Grains weighing 30.1 mg in total were selected for K-Ar work. These were crushed in a small mortar under distilled water. The resulting powder was treated for 40 minutes with 0.1 M hydrochloric acid and then separated from the liquid by centrifuging and decantation. The powder was washed twice with ethanol (decanted away after centrifuging) and finally dried at 50°C.

The dried glauconite powder was weighed into a copper-foil capsule, which was then closed by folding. The folded capsule and a small fused-quartz test tube were placed inside a horizontal glass tube that included a section of fused-quartz glass. The horizontal tube, part of a vacuum line for argon extraction, was then sealed by glassblowing. After overnight evacuation, the central part of the fused-quartz section of the horizontal tube, where the sample was to be heated, was pre-heated for twenty minutes with a small external electrical resistance heater to a temperature near 1100°C. The fused-quartz test tube was then moved into the pre-heated area and heated by the protocol used later for heating the glauconite. This heating of the empty test tube yielded a small amount (0.25 pmol) of argon having the isotopic composition of atmospheric argon. The copper-foil capsule containing the glauconite was then moved into the fused-quartz test tube and placed at its closed end, and the external heater

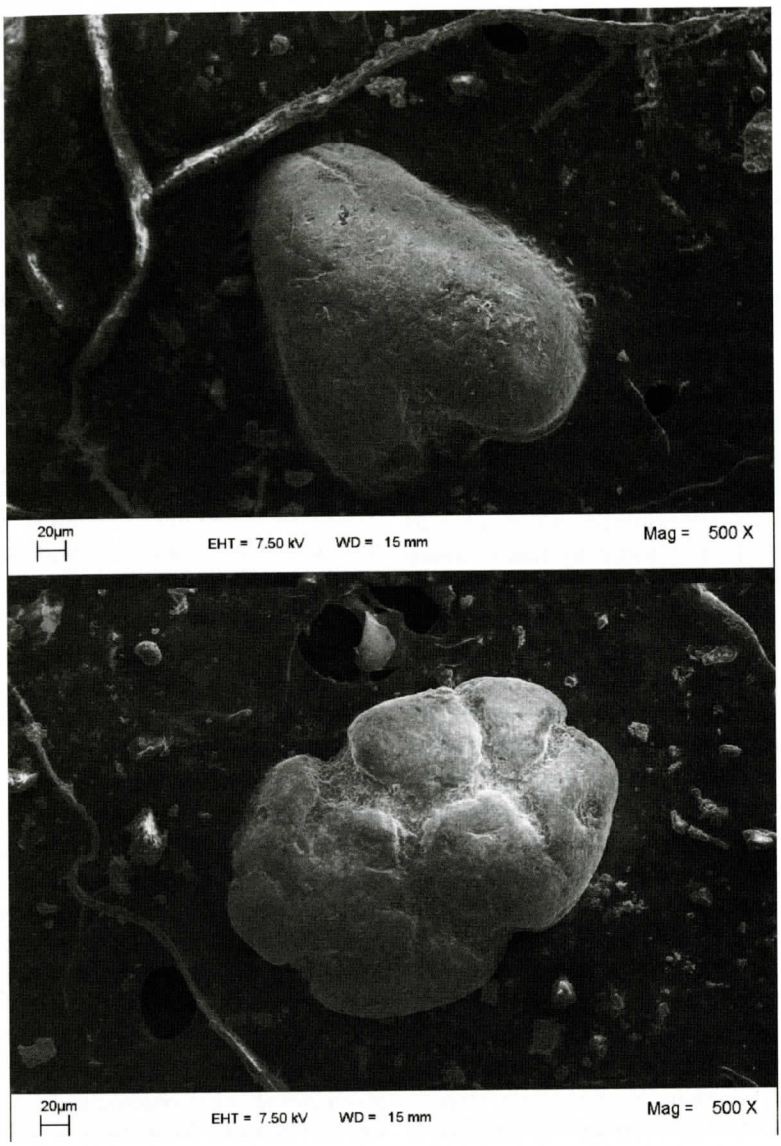

Figure 3: SEM images of representative grains separated by hand for K-Ar measurements.

was centered over the capsule. Power was brought up gradually over 15 minutes and held constant for an additional 7 minutes at a value expected to hold the capsule at a temperature between 1000°C and 1050°C. The actual temperature of the capsule exceeded 1050°C and the copper melted, but the heated (partially melted) powder was retained in the closed end of the fused-quartz test tube. Any potassium evaporated during heating would have condensed in a cooler portion of the fused-quartz test tube that extended beyond the heater. The gases released by heating the glauconite were mixed with a known amount of ^{38}Ar. After less-volatile gases had been removed from the mixture in cold traps, heated titanium in two stages was used to remove reactive gases. The isotopic composition of the argon (a mixture of argon from the sample and the added ^{38}Ar) was measured with an AEI Model MS-10 mass spectrometer attached to the argon extraction line.

The test tube containing the residual solid

was then removed from the argon extraction line and its contents (copper, the silicate residue of the glaucony, and any potassium that may have evaporated from the silicate residue) were transferred with a 10:1 mixture of hydrofluoric acid and perchloric acid into a fluorocarbon (FEP) container. Nitric acid was added to fully dissolve the copper, and the FEP container was closed and heated gently overnight to digest the silicate residue. Then the FEP container was opened and heated more strongly to drive off excess acid and SiF_4. The residual solids were taken up in a measured amount of an acidic (0.1 mol/kg nitric acid) cesium chloride (0.01 mol/kg) solution. After further dilution with the same solution, the mass fraction of potassium in the solution was determined in reference to standard potassium solutions by flame atomic absorption spectrophotometry (FAAS) with a Perkin Elmer Model 3100 spectrophotometer.

Because the silicate residue had reacted slightly with the test tube, the inside of the tube was washed (etched) several times with the hydrofluoric-perchloric acid mixture to extract potassium that had diffused into the fused-quartz glass. During each wash, the hydrofluoric acid was allowed to dissolve silica from the inner walls of the tube for about 15 minutes. Each wash solution was transferred to its own FEP container and evaporated to dryness. The residues were taken up in measured small amounts of the acidic CsCl solution for potassium determination by FAAS. Small but significant amounts of potassium were found in the first two wash solutions (8 μg and 7 μg, respectively, out of 1010 μg total for the glaucony). The third wash solution had virtually no potassium (1 μg), so no further washes were done.

Subsequent work (to be published elsewhere) with other glaucony samples, including the interlaboratory reference sample GL-O, has confirmed that >99.8% of the argon in well-evolved glaucony is extracted when it is held for 10 minutes between 1000°C and 1050°C and that >99.95% of the potassium remains within the copper-foil capsule (which does not melt in that temperature range).

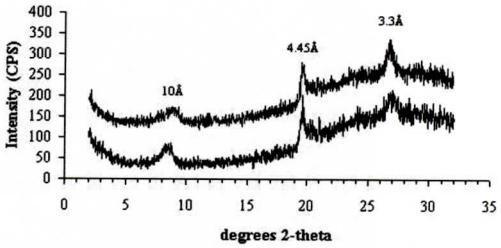

Figure 4: Diffraction patterns of the powdered glaucony. The upper pattern shows the diffraction pattern after solvation with ethylene glycol vapor. The lower pattern shows the diffraction pattern after drying in air. The presence of glauconite is based on the presence of the peaks at 10 Å and at 3.3 Å and the absence of a peak at 5 Å (17.7° 2θ).

RESULTS

Glaucony grains usually range in color from yellow-green to dark green, however, the grains selected for K-Ar measurements and mineralogic characterization were the dark green variety, 2.5/2 5G, 3/2 5G, and 2.5/1 5G on the Munsell Color Chart. These grains were dark grayish green and greenish black and were botryoidal in habit (Figure 3). The grains ranged from 0.15 mm to 1.0 mm in diameter along the longest axis. Before crushing and reaction with 0.1 M HCl, the glaucony grains selected for the K-Ar work had a mass of 30.1 mg. Afterward, the mass of the remaining powder was 18.1 mg. More of the dark green grains described above, about 20 mg, were crushed and analyzed by X-ray diffraction. Glauconite was the primary mineral observed from X-ray diffractometry (XRD) analyses. The XRD scans of both air-dried and glycol-solvated oriented mounts show the presence of a broad 10 Å peak and a more intense 3.3 Å peak and the absence of a 5 Å peak (Figure 4). The peak at 4.45 Å near 20° 2θ is a characteristic *hkl* reflection for phyllosilicates. The background intensity increases from 20° 2θ to the end of the scan at 32° 2θ due to scatter from the glass slide. The age calculated from measurements of potassium and argon isotopes in the glauconite is 33.7 ± 1.0 Ma (Table

Table 1: Results of Potassium-Argon Measurements of Glauconitic Grains from the Ocmulgee Limestone.

Sample Mass (mg)	K (µg)	K (% by mass)	$^{40}Ar^*$ (% of ^{40}Ar)	$^{40}Ar^*$ (nmol kg^{-1})	K-Ar Age (Ma)
18.09	1010†	5.58† ± 0.06‡	73	325 ± 9‡	33.7 ± 1.0‡

* The symbol $^{40}Ar^*$ stands for radiogenic argon.

† Includes 16 µg of potassium etched from the fused-quartz test tube in three washes.

‡ Uncertainty ranges are based on estimates of the analytical error at the 95% confidence level (2σ).

1). The amount of potassium used in calculating the age includes 16 µg of potassium from the three washes (etches) of the fused-quartz test tube, since that potassium is assumed to have entered the glass by reaction of the glaucony residue with the glass. The 1.0 Ma uncertainty is an estimate of the effect of analytical error on the age value at the 95% confidence level (2σ). The argon isotopic composition shows a high percentage of radiogenic argon ($^{40}Ar^*$), 73%. The K content of the glauconite powder was 5.58 weight percent (6.72 wt.% K_2O).

INTERPRETATION AND DISCUSSION

The presence of 10 Å diffraction peaks and the absence of 5 Å diffraction peaks on XRD scans of both air-dried and glycol-solvated glaucony powder indicate the presence of glauconite within the glaucony grains separated from the Ocmulgee Limestone. The increase in background intensity between 20° and 32° 2θ is interpreted to represent scatter of X-rays from the glass slide and/or the presence of amorphous matter within the grains. In aggregate, grains composed of glauconite can be considered to be "evolved" glaucony. Given that the time required for evolution of glaucony is typically 10^4-10^5 years (Odin and Matter, 1981), the 33.7 ± 1.0 Ma age value of the glaucony grains is interpreted to date the deposition of the upper portion of the Ocmulgee Limestone collected in this study. This interpretation assumes that these glaucony grains are authigenic rather than epiclastic. As shown in Figure 5, the numerical age range 32.7 Ma to 34.7 Ma for the glaucony grains is consistent with the latest Eocene (Jacksonian) age for the Ocmulgee Limestone proposed by Huddlestun and Hetrick (1986) and also with the early Oligocene biostratigraphic age proposed by Pickering (1970). Insofar as the analytical errors are random, the most probable value within that range is the central value 33.7 Ma, which is close to the currently accepted date of 33.9 ± 0.1 Ma for the Eocene-Oligocene transition (Luterbacher and others, 2004). Additional K-Ar analyses of glaucony grains are needed from throughout the Ocmulgee Limestone to refine further the range of depositional ages of the Ocmulgee Limestone in central Georgia.

The K-Ar age for the glaucony grains from the Ocmulgee Limestone is in accord with other radiometric ages from rocks in the region. The central value, 33.7 Ma, is 0.6 Ma less than that for the K-Ar age of dark green glaucony grains (34.3 ± 0.4 Ma) from the underlying Twiggs Clay Member of the Dry Branch Formation reported by Albin and Wampler (1996). The difference is not statistically significant, but it is large enough to suggest that a numerical age difference consistent with the difference in stratigraphic position could likely be confirmed with more precise measurements. The K-Ar age obtained in this study is also consistent with the age inferred for a thin sand layer at the base of the Twiggs Clay Member that contains shocked quartz grains thought to have been ejected from the Chesapeake Bay impact event (35.7-36.0 Ma, Harris and others, 2004).

This work also shows that it is possible to obtain an accurate K-Ar age using the methods described herein. Despite the small sample mass of 18 mg, the amounts of radiogenic argon and potassium in that sample were sufficient for accurate measurements. The error for the K-Ar age is lessened by use of one weighing (Dalrymple and Lanphere, 1969), because sample inhomogeneity does not contribute to error in

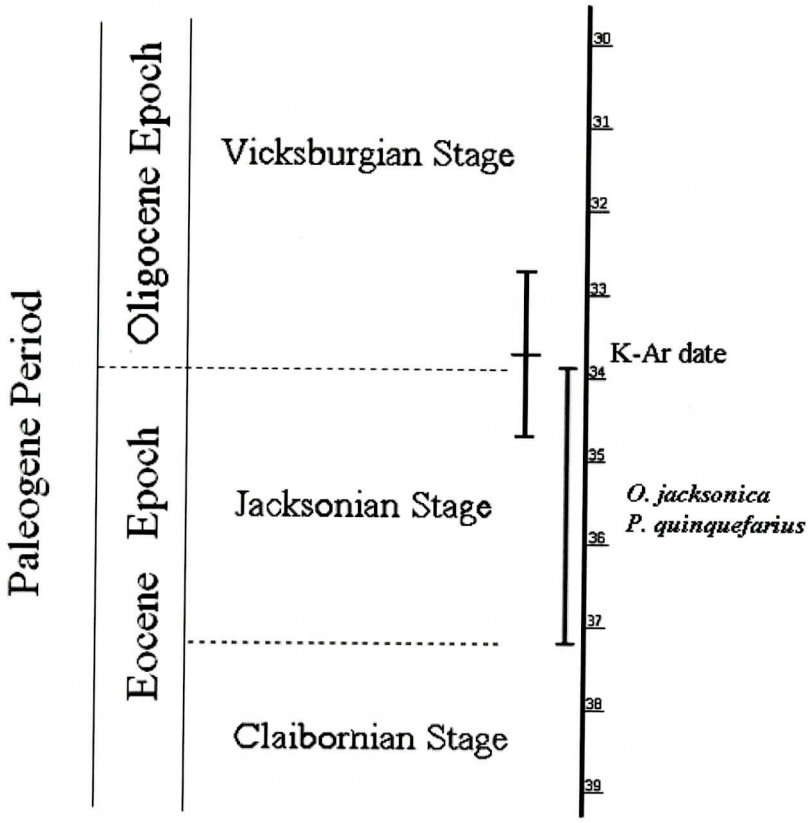

Figure 5: Geologic time scale showing numerical ages of relevant stages of the Eocene and Oligocene epochs, the known ranges of *O. jacksonica* and *P. quinquefarius* (spanning the Jacksonian Stage), and the K-Ar age (33.7 ± 1.0 Ma) of glauconite from the Ocmulgee Limestone.

the age value, nor does any error in weighing. The method described herein makes possible the determination of K-Ar age values where only small amounts of glauconite are available.

CONCLUSIONS

Dark green grains found in the Ocmulgee Limestone are identified as being composed of glauconite, and this glauconite contains sufficient potassium and radiogenic argon for good K-Ar measurements. The external appearance and the potassium content of the grains are those of evolved glaucony. The material remaining after argon extraction was used for the potassium measurement, a method that requires only a small amount of sample and provides a K-Ar age value unaffected by sampling error and weighing error. These results indicate that the interval of the Ocmulgee Limestone studied herein was deposited 33.7 ± 1.0 million years ago. This K-Ar age places the depositional age of the layers studied near the Eocene-Oligocene boundary of 33.9 ± 0.1 Ma (Luterbacher and others, 2004). This age is also consistent with a recently determined K-Ar age value for dark green glaucony from the underlying Twiggs Clay Member of the Dry Branch Formation. This result raises a question regarding the range of depositional ages represented by the Ocmulgee Limestone and its characteristic fossil assemblages (e.g. *Ochetosella jacksonica*) in the Georgia Coastal Plain.

ACKNOWLEDGEMENTS

This project was sponsored by the Atlanta Consortium for Research in the Earth Sciences

(ACRES) which was funded by the National Science Foundation (grants EAR-9820666 & EAR-0139539) to Georgia State University (Prof. Pamela C. Burnley, Primary Investigator). Dr. Robert Simmons (Georgia State University Department of Biology) provided the SEM images of the glaucony grains. We thank Scott Harris for helpful discussions prior to the writing of this manuscript and Tim Chowns for a helpful review of an earlier version of the manuscript.

REFERENCES CITED

Albin, E.F., and Wampler, J.M., 1996, New potassium-argon ages for georgiaites and the upper Eocene Dry Branch Formation (Twiggs Clay Member): Inferences about tektite stratigraphic occurrence. *in*: Abstracts of the 27th Lunar Planetary Science Conference, Houston Texas, Lunar Planetary Institute, p. 5-6.

Bailey, S.W., Brindley, G.W., Kodama, H., Martin, R.T., 1979, Report of the Clay Minerals Society Nomenclature Committee for 1977 and 1978: Clays and Clay Minerals, v. 27, p. 238-239.

Bornhold, B. and Giresse, P., 1985, Glauconitic sediments on the continental shelf off Vancouver Island, British Columbia, Canada: Journal of Sedimentary Petrology, v. 55 no. 5., p. 653-664.

Canu, F. and Bassler, R.S., 1920, North American Early Tertiary Bryozoa: United States National Museum Bulletin, v. 106, 879 pp.

Dalrymple, G. and Lanphere, M., 1969, Potassium Argon Dating: Principles, Techniques and Applications to Geochronology: W.H. Freeman and Sons, New York.

Evernden, J.F., Curtis, G.H., Obradovich, J.D., Kistler, R.W., 1961, On the evaluation of glauconite and illite for dating sedimentary rocks by the K-Ar method: Geochimica et Cosmochimica Acta, v. 23, p.78-99.

Harris, L. and Whiting, B., 2000, Sequence-stratigraphic significance of Miocene to Pliocene glauconite-rich layers, on- and offshore of the US Mid-Atlantic Margin: Sedimentary Geology, v. 134, p. 129-147.

Harris, R.S., Roden, M.F., Schroeder, P.A., Holland, S.M., Duncan, M.S., Albin, E.F., 2004, Upper Eocene impact horizon in East Central Georgia: Geology, v. 32, p. 717-720.

Harris, W.B., and Bottino, M.L., 1974, Rb-Sr study of Cretaceous lobate glauconite pellets, North Carolina: Geological Society of America Bulletin, v. 85, p. 1475-1478.

Harris, W.B., and Fullagar, P.D., 1989, Comparison of Rb-Sr and K-Ar dates of middle Eocene bentonite and glauconite, southeastern Atlantic Coastal Plain: Geological Society of America Bulletin, v. 101, p. 573-577.

Huddlestun, P., 1993, A Revision of the Lithostratigraphic Units of the Coastal Plain of Georgia: The Oligocene: Bulletin Georgia Geological Survey, v. 105, p. 16-19

Huddlestun, P. and Hetrick, J, 1986, Upper Eocene Stratigraphy of Central and Eastern Georgia: Bulletin Georgia Geological Survey, v. 95, p. 53-54.

Hurley, P.M., Cormier, R.F., Fairbain, H.W., Hower J. Jr., Pinson, W.H., Jr., 1960, Reliability of glauconite for age measurement by K-Ar and Rb-Sr methods: Bulletin of the American Association of Petroleum Geologists, v. 44, p. 1793-1808.

Lipson, J., 1958, Potassium Argon dating of sedimentary rocks: Bulletin of the Geological Society of America, v. 69, p. 137-150.

Luterbacher, H.P., Ali, J.R., Brinkhuis, H., Gradstein, F.M., Hooker, J.J., Monechi, S., Ogg, J.G., Powell, J., Rohl, S., Sanfilippo, Schmitz, B., 2004, The Paleogene Period. *in*: Gradstein F.M., Ogg, J.G., and Smith, A.G. eds., A Geologic Time Scale, Cambridge University Press, p. 384 -408.

Moore, D.M., and Reynolds, R.C., Jr., 1997, X-ray diffraction and the identification and analysis of clay minerals. Oxford University Press, New York, 378 pp.

Odin, G.S., 1982a, How to measure glaucony ages. *in*: Odin G.S. ed., Numerical Dating in Stratigraphy. John Wiley and Sons, p. 387-403

Odin, G.S., 1982b, Effect of pressure and temperature on clay mineral K-Ar ages. *in*: Odin G.S., ed., Numerical Dating in Stratigraphy. John Wiley and Sons, p. 307-319.

Odin, G.S. and Matter, A., 1981, de glauconiarum origene: Sedimentology, v. 28, p. 611-641.

Odin, G.S, and Velde, B., 1975, Further information related to the origin of glauconite: Clays and Clay Minerals, v. 23, p. 376-381.

Odin, G.S., Velde, B., Bonhomme, M., 1977, Radiometric argon in glauconies as a function of mineral recrystallization: Earth and Planetary Science Letter, v. 37, p. 154-158.

Pickering, S. Jr., 1970, Stratigraphy, paleontology, and economic geology of portions of Perry and Cochran quadrangles, Georgia: The Geological Survey of Georgia Department of Mines, Mining and Geology, v. 81, 67 p.

Suurmeyer, N. R., Howell, E., Powell, R.D., Smith, A. M., Anderson, J.R., Young, C.G., Elliott, W. C., 2003, Microfacies correlation of the Upper Eocene Sandersville Limestone member of the Tobacco Road Sand to the Ocmulgee Formation on the Coastal Plain of Georgia, Abstracts with Programs, Geological Society of America, v. 34, n. 7, p. 192.

Thompson, G.R., and Hower, J., 1973, An explanation for low radiometric ages from glauconite: Geochimica et Cosmochimica Acta, v. 37, p. 1473-1491.

Wasserburg, G.J., Hayden, R.J., Jensen, K.J., 1956, ^{40}Ar-^{40}K Dating of Igneous Rocks and Sediments: Geochimica et Cosmochimica Acta, v. 10, p. 153-165.

Wortman, S. R., Stephens, E., Lawrie, K., Burger, E. Gullett-Young, C., Foote, J., Anderson, J.R., Elliott, W. C., 2004, Correlation of Upper Three Runs aquifer to the Eocene Sandersville Limestone, Coastal Plain, Geor-

gia, Abstracts with Programs, Geological Society of America, v. 36, n. 5, p. 80.

SOUTHEASTERN GEOLOGY
V. 45, No.1, June 2007, p. 25-42

AN EVALUATION OF BEACH RENOURISHMENT SANDS ADJACENT TO REEFAL SETTINGS, SOUTHEAST FLORIDA

HAROLD R. WANLESS AND KATHERINE L. MAIER[1]

Department of Geological Sciences
University of Miami
PO Box 249176
Coral Gables, FL 33124

[1]*now at Department of Geological and Environmental Sciences, Stanford University, Stanford, CA 94305*

ABSTRACT

Most sediment chosen for southeast Florida beach renourishment projects displays unsuitable grain size, durability, and hydrodynamic behavior for a beach setting. As a result, the coral and hardbottom communities lying on the adjacent narrow shelf are being stressed by increased sediment turbidity, siltation, and smothering. Historical and proposed renourishment sands derived from dredging on the adjacent shelf contain excessive amounts of fine sand and silt too small to remain on the beach, resulting in persistent long-term suspension-transport release to nearshore waters. Most shelf-derived renourishment sands contain much less durable carbonate skeletal material than the natural beach sands, when tested in a tumbling barrel designed to reproduce natural beach abrasion. In addition, carbonate skeletal grains display hydrodynamic behavior of grain sizes smaller than their sieve sizes when settled in a vertical accumulation tube. When used for renourishment, a higher percentage of these sands will not remain on the beach. Durability and wet settling analyses must be utilized in evaluating sediment for possible placement on a beach.

Failure to use sand of proper size, behavior, and durability in beach-fill projects results in decreased project life and long-term degradation of the adjacent sandy and hardbottom communities and coral reefs.

INTRODUCTION

Coral and hardbottom communities thrive on the linear limestone ridges along the narrow continental shelf off the coast of southeastern Florida (Figure 1). These communities require clear water, low turbidity, low nutrients, and low incidence of siltation and smothering. Benthic habitat biologists (Nelson, 1989; Wilber and Stern, 1992; Hughes and Connell, 1999; Peterson and others, 2000; Bush and others, 2004), coastal fisheries scientists (Hackney and others,1996; Lindeman and Snyder, 1999), recreational fishers and sport divers are reporting a progressive degradation of hard bottom and fish communities along the inner shelf of southeastern Florida. Monitoring designed to assess the impact on these valuable biologic resources often does not meet scientific standards (Peterson and Bishop, 2005). It is the purpose of this paper to assess the role that current beach management and dredge and fill practices may be playing in environmental degradation.

Beach renourishment, also known as dredge and fill, has become a common treatment for the erosion occurring along up to 90% of U.S. sandy shorelines (Davidson and others, 1992; Blott and Pye, 2004). Jetties, groins, seawalls, artificial inlets and other man-made physical structures intended to protect shorelines and enhance habitation have disrupted the natural flow of sand along the coast and led to significant erosion (Newman, 1976; Pilkey, 1983; Galvin, 1990; Nordstrom, 2000). This erosion is now enhanced by a dramatic increase in the rate of relative sea level rise since 1930 (Wanless and others, 1994; Zhang and others 1997, 2000).

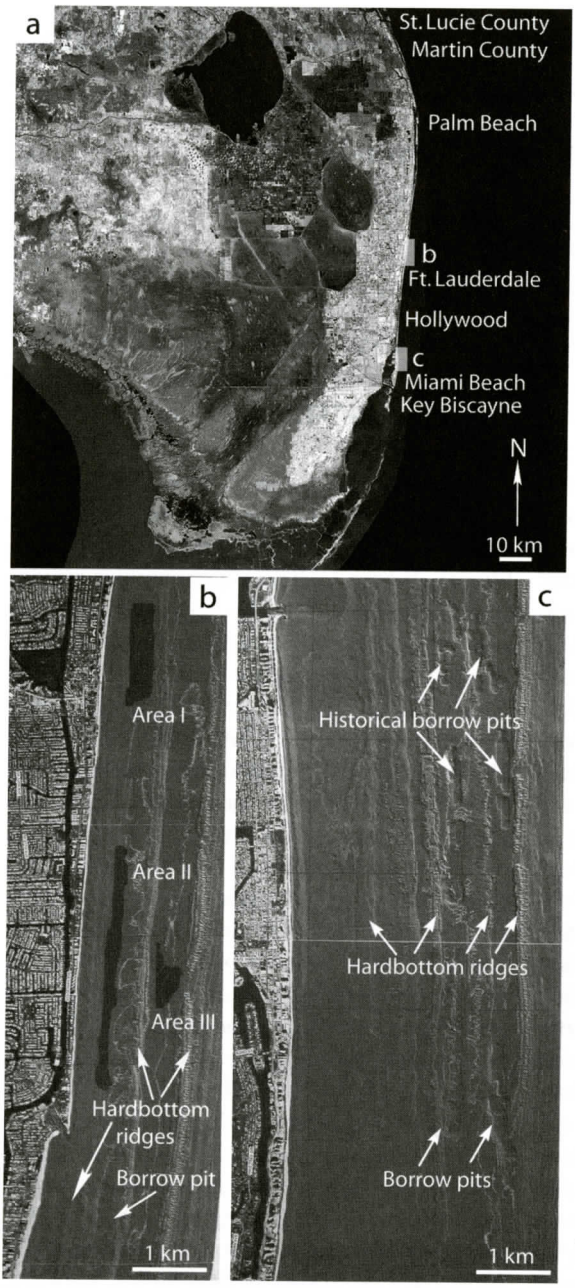

Figure 1. A. Satellite image of south Florida showing locations of beach fill activities discussed in this paper. Port Everglades Inlet Channel is between Dania and Ft. Lauderdale. B. Proposed offshore areas for dredging sand for placing on northern Broward County beaches are superimposed on a Laser Airborne Depth Sounding (LADS) sun shaded bathymetry image. Hardbottom communities and coral live on limestone ridges between proposed dredge sites. C. LADS image of the shelf off of northern Miami Beach showing offshore borrow pits from early 1980s beach fill project. Images produced by Broward County (B) Miami-Dade County (C), Florida Department of Environmental Protection and US Army Corps of Engineers.

This erosion and increasing ocean-front development and tourism have prompted increasing beach renourishment projects along the southeastern Florida coast.

However, the distribution of sediment in the beach profile and its transportation is not governed entirely by physical grain size. Factors such as density, mineralogy, shape and surface texture also affect a grain's hydrodynamic behavior (Zeigler and Gill, 1959). Settling analysis through a column of water can be used as a measure of how beach sand grains will behave. Sengupta and Veenstra (1968) advocate the use of settling velocity as an additional grain parameter because it demonstrates grain behavior under natural conditions more accurately than sieve analysis alone. Settling behavior is important not only for fine grains that travel in suspension, but also for bedload sizes because traction is affected by the same shape and density factors (Braithwaithe, 1973). It is especially important to consider grain behavior in South Florida where a large component of the sand is carbonate skeletal grains.

Durability of the sand is also important in governing the success of a beach renourishment project. Many of the same factors considered in hydrodynamic behavior, such as shape and density, must also be considered for durability. Sediments on natural beaches have usually experienced considerable reworking (Riddell and Young, 1992), whereas the calmer offshore borrow areas are likely to have accumulated skeletal sediment without a history of abrasion. Few studies have investigated the durability of beach sediment.

This article discusses the fundamentals of sand that pertain to beaches, and then evaluates the quality of sand fill for recently completed and for planned projects

along the Atlantic coast of central and south Florida. Specifically, it focuses on the transport behavior and durability of calcium carbonate skeletal grains, as these are an important component of many proposed sources for obtaining beach fill.

BACKGROUND: THE FUNDAMENTAL PROPERTIES OF SAND

Four fundamental properties of sand particles must be addressed in considering sediment for beach fill – size, density, shape and durability. Beaches on the Atlantic and Gulf Coast of the United States are primarily made of grains of quartz and grains of calcium carbonate skeletal fragments. Quartz sand is the standard from which sands are considered.

Quartz Sand Dynamics

Quartz sand is derived from the weathering of continental igneous and metamorphic rocks. It has a density of 2.65, is solid mineral material, and has a hardness of seven. By the time it has been eroded from the source rock and traveled down rivers and along the shore to a given beach, quartz grains are generally equant in shape and sub-rounded to well-rounded. As quartz is gradually added to the beach system, the grains continue to become more rounded and commonly polished or frosted. The beach is an effective abrasive environment, with the constant energy of breaking waves and beach swash. A great amount of literature is devoted to characterizing the entrainment, transport, and depositional behavior of quartz sands. Most research on quartz has used grain-size analysis by sieving as a basis for calibration of size versus sediment dynamics.

There are three important features of the dynamics of quartz sand. First, quartz grains that are finer than 200 microns will tend to move in suspension. Bagnold (1966), working on desert dunes, and McCave (1970), working in the marine waters of the North Sea, have both shown that when there is enough energy to move particles less than 200 microns, there is enough fluid

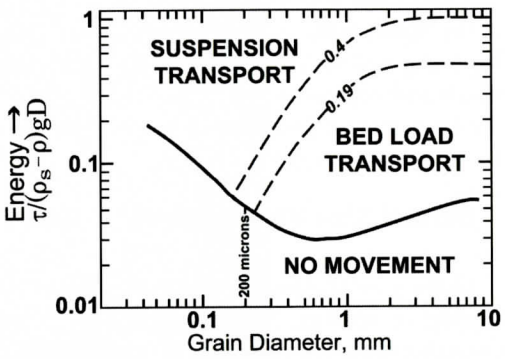

Figure 2. Entrainment diagram for quartz sands. When there is sufficient wave or current energy to move grains finer than 200 microns, then there is also enough turbulence to transport them in suspension (τ=shear stress; ρ_s=density of grain; ρ=density of fluid; and D=grain diameter). Modified from McCave 1970.

turbulence to move these particles in suspension (Figure 2). Sand less than 200 microns will not remain in settings where there is frequent energy for movement – such as in the beach and nearshore zone. With increasing prevailing energy, coarser and coarser particles will move in suspension and be removed from the beach zone.

Second, Passega and others (1967), using data from the Mississippi River and the Adriatic Shelf, have shown that suspension transported particles can be divided into short-term suspension and long-term suspension. Particles about 30 to 200 microns in size will settle out after the transporting energy event is over or is no longer acting on the bottom (short-term suspension). Ambient turbulence in the water column will keep particles finer than about 30 microns in suspension long after the transporting energy event is over (long-term suspension). When applied to sediment placed on beaches, erosion and transport of less than 200 micron sediment will move and deposit sand as two populations. The short-term suspension (30-200 micron) grains will accumulate and result in siltation on the adjacent inner shelf bottom below prevailing condition wave base. The long-term suspension (less than 30 micron) grains will remain in the water column for long periods, reducing water clarity over a broad area across the shelf.

Third, sand that is of suitable size to remain in the beach zone will transport as a bedload, bouncing and sliding up, down and along the beach and nearshore zone. Bedload transport results in intense grain abrasion in the breaking wave and swash zone.

Sieved Size Versus Settling Size

Grain size analysis can be made either by sieving or settling. Sieving separates grains through a stack of decreasing mesh sieves and is a measure of the two smaller dimensions of a grain. For equant, solid quartz grains, sieving is a fair measure of its three dimensional character, but for skeletal sands, sieving can give a very misleading result (Figure 3).

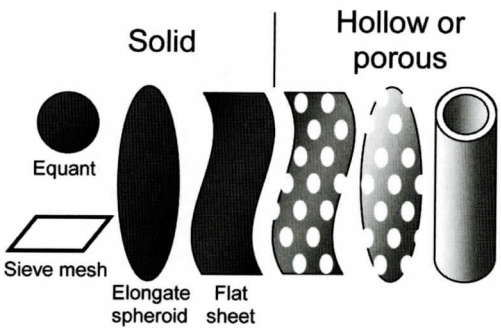

Figure 3. Sieve analysis of sand size measures the two shorter axes of a grain. For equant quartz grains, sieving provides a good measure of particles of similar mass and hydrodynamic behavior. In sand with large amounts of carbonate skeletal grains, sieving may group together grains of many different sizes, shapes, and effective densities.

Some carbonate skeletal grains (molluscs) and non-skeletal grains (ooids) consist of quite densely arranged crystals and have an effective density similar to quartz. Most carbonate grains have unusual shapes (platy, elongate), are hollow or very porous, and/or have pronounced surface irregularities (spines or bumps). Hollow or porous grains will have a much lower effective excess density than a solid mineral grain (like the difference between a golf ball and a ping-pong ball). Shape, internal porosity and surface ornamentation will all affect how carbonate grains behave on a beach.

Settling analysis avoids the misleading results of sieving by separating grains only based on their hydrodynamic behavior. Effective size is evaluated by comparing a sample's settling time through a vertical accumulation tube (Subcommittee on Sedimentation, 1957) with the time for an equant quartz grain standard. Platy and porous carbonate grains will be assigned a much smaller grain size through settling than through sieving analysis.

Particle Shape

Many carbonate skeletal grains are platy in nature. This affects not only their settling behavior (like a dropped piece of paper) but also their ease in entrainment and transport behavior. Platy grains move more easily than equant grains with which they group by sieving analysis (Figure 3). In addition, thin platy carbonate grains are easily broken in the surf and swash zone of the beach. Platy grains are easily entrained and kept moving by bottom currents. Flat and curved platy grains are very common in carbonate sands offshore south Florida's beaches. Although there is no standard analysis for platy grain behavior, their abundance can easily be quantified by examination of the sand fractions with a binocular microscope. The platy, skeletal grains should be subtracted from the useful sand in evaluating potential beach fill material.

Particle Durability

Quartz sand grains are mostly single crystals with few internal planes of weakness and a hardness of 7. Carbonate skeletal grains are composed of many small crystals, organic films, and open pore spaces. Calcite and aragonite, the minerals making up carbonate skeletal grains, have a hardness of 3. Skeletal carbonate grains that are thin and platy or that have a porous internal structure are likely to be less durable in a beach setting.

In addition, carbonate grains are commonly substrates into which micro-organisms bore, creating open holes. Cyanobacteria and fungi bore into carbonate particles lying on the sea floor in areas that are not highly energetic day to day. Carbonate skeletal gravel lying on the

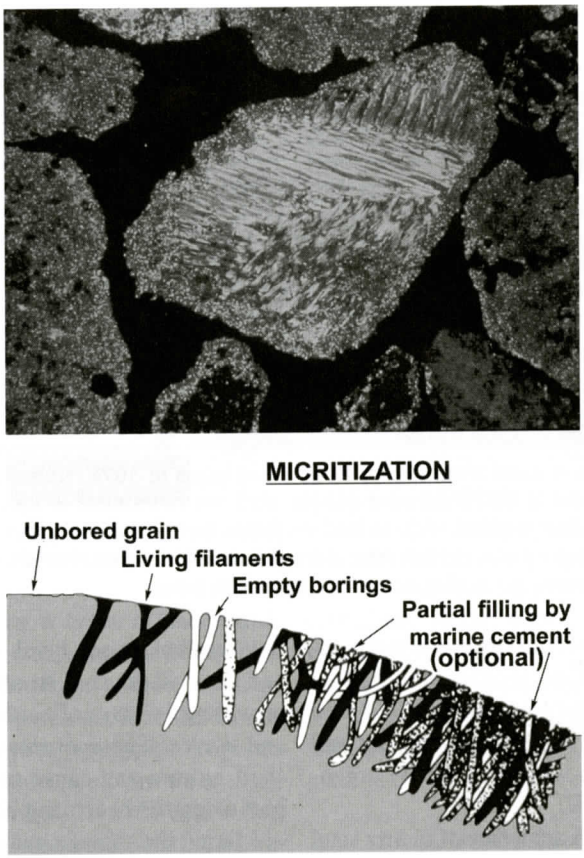

Figure 4. Top—Thin section photomicrograph of a mollusc fragment. Original crystalline microstructure of mollusc has been destroyed in outer portion by micritization. Other grains have been completely micritized. If placed in an agitated abrasive environment, the outer portion of the grain will quickly be eroded. Grain is 650 microns in long dimension. Bottom—Sketch of cyanobacterial microborings on carbonate grain surface. Microborings may penetrate 50-100 microns into a grain, weakening the structure. (Modified from Kobluk, 1977.)

sea floor may additionally be intensely bored by endolithic sponges, barnacles, and molluscs. On death of the boring microbes, fine marine carbonate cement may precipitate, loosely filling the borings. This grain alteration by microboring and fine cement infilling is termed micritization (Figure 4). Cement infilling may not occur. Boring and microboring greatly weakens the surficial portion of the grains. The boring/micritized zone generally extends 50-100 microns into the grain, but some grains become pervasively bored.

To illustrate the importance of these fundamentals of sand behavior, an evaluation of used and proposed beach renourishment sands from areas containing other than pure quartz sands is presented. These are beach renourishment projects along the east coast south Florida between St. Lucie and Miami-Dade Counties.

SETTING

Southeast Florida has a continuous string of narrow sandy barrier islands bordering a narrow continental shelf (Figure 1). The shelf and shore is increasingly protected from oceanic swells to the south by the Bahama banks. The shelf ranges from 3 to 8 kilometers in width and deepens from the shore to about 30 m depth at the margin. The shelf contains a series of 2-4 linear

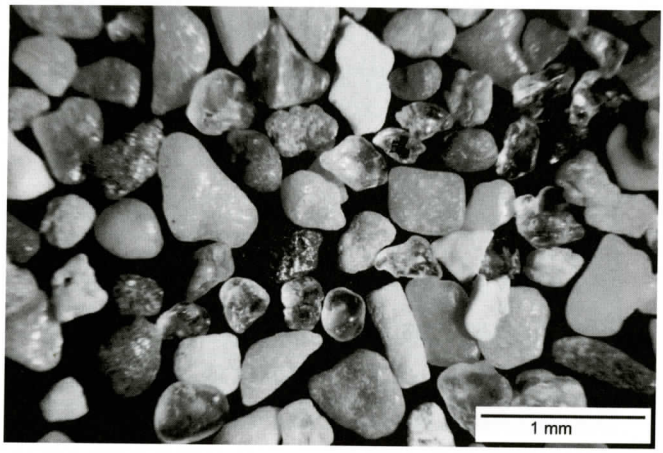

Figure 5. Natural beach sand from Miami Beach collected in 1976. Natural beach sand on the southeast Florida coast is 25-75 percent quartz, and the remainder is carbonate skeletal fragments. The quartz is clear, equant, sub- to well-rounded and polished by beach abrasion. The carbonate skeletal grains are cream to tan robust fragments of mollusc shell that have been rounded and polished as they were gradually added to the beach zone.

shore-parallel ridges of limestone and intervening troughs. Ridges have prolific hard bottom and reefal communities; troughs are filled with as much as 10 meters of skeletal sand, silt and gravel, most of which was produced by organisms living on the shelf.

The natural beaches are a mix of quartz sand and skeletal carbonate sand. Quartz sand is primarily in the 200-500 micron size range, other sizes being selectively removed during transport from the source of the southern Appalachian Mountains. Coarser-grained beaches and beach zones are thus predominantly skeletal carbonate. Medium-grained beaches and beach zones are as much as 75% quartz. The skeletal component of natural beach sand is predominantly rounded and polished fragments of molluscs (Figure 5).

Offshore of the beaches of southeast Florida, the sand surface slopes to 5-15 meters depth where it intersects the hard Pleistocene limestone surface. Sand filling the more nearshore troughs is in part derived from the beach environment. Sand filling the more seaward depressions is nearly entirely carbonate skeletal sand, which has never been associated with a beach environment.

Prevailing winds are from the southeast and gentle. Fair weather wave base is thus only a few feet below sea level. Between November and May 40-60 cold fronts pass through, each providing 1-3 days of north and northeast winds and waves. These events agitate the offshore shelf bottom and cause southward sand transport along the beach and nearshore zone. North of Miami, the shore is increasingly open to oceanic swells from the open Atlantic. Winter cold fronts and oceanic swells cause a net southward transport of sand along the beach and nearshore zone. Estimates range from 80,000 to 300,000 cubic yards of sand moving southward past a point each year.

Tropical storms and hurricanes also affect south Florida beaches. A segment of coast receives hurricane force winds on the average of once every 7.5 years, yet slow moving tropical storms can also cause serious erosion. Severe weather that creates a flood storm surge washes sand from the beach onto or across the sandy barrier islands.

A dramatic increase in the rate of relative sea level rise began about 1930 and is continuing. To date, south Florida has experienced a 23 cm rise since 1930, at a rate 8 times the average for the past 2,000 years (Wanless and others, 1994). This rapid rise has destabilized the equilibrium profile of the beaches, exposed the shore to less attenuated wave energy, and

caused more frequent storm overwash onto the barrier islands (Zhang and others, 1997, 2000).

METHODS

Field

Beach sand samples from natural beaches were collected from the beach slope at 0-20 cm from the surface. Sand from beaches that have received sand fill was collected by digging into the back beach fill below a zone of post-placement reworking. Generally 4-6 separate samples are collected and mixed to provide a composite fill sample. Unusually coarse or fine fill zones are avoided as are mud lumps. Collection of sands from recent beach fill projects in Martin and St. Lucie Counties occurred in the spring of 2005.

Proposed sand borrow areas offshore Broward County beaches were sampled from vibracores collected by the senior author. As these were collected under permission of the Court, only 50 ml samples were permitted. Proposed borrow area sand samples are from three sites. Sites I and II are the sand fill in the depression between the first and second offshore limestone ridges seaward of the beaches of northern Broward County (Figure 1). Proposed Site III is between the second and third offshore limestone ridges. In Broward County, sand from two beach transects was collected in the spring of 2005 from natural beaches north of Port Everglades.

Sand samples from Miami Beach's natural and renourished beaches were collected in 1976, 1981 and 2005. Sand from Key Biscayne was collected at various times between 1975 and 2005, including following the 1985 placement of beach fill. Samples were generally taken from the back beach, the berm crest, the beach slope, and offshore below the low tide plunge line.

Sieving and Settling

All samples were first rinsed with tap water to remove excess salts. Samples without any mud content were dried in an oven at 80°C in preparation for dry sieving, while samples having any mud fraction were kept wet and refrigerated. A fraction of the wet samples was sieved to remove the less-than-62 micron fraction. Drying samples with significant mud content will result in cementation and unnatural grain aggregations (Wanless and others, 1981). The coarser fraction was then dried in preparation for dry sieving through a stack of phi-interval mesh sieves using a Ro-Tap Shaker.

A visual accumulation tube (Subcommittee on Sedimentation, 1957) was utilized to measure and observe the settling behavior of each sample and how settling size differed from sieve size distribution. Settling time of each sample was translated into a grain size distribution by calibration with a standard of equant, sub-rounded quartz. Changes in composition with settling size were observed as sediment accumulated in the narrow bottom of the tube. Five samples were submitted to an independent sedimentology laboratory at Indiana University/Purdue University at Indianapolis for settling with no indication as to the nature of the samples.

Durability Analysis

Rolling Stones Rock Tumblers were used to simulate abrasion on the beach plunge/swash zone. These tumblers are three-inch diameter plastic canisters with small linear ridges inside to disrupt the particles' movement along the wall. They rotate at 60 rpm. Between seven and a half and fifteen and a half grams of sand, an equal weight of 'abrasive,' and 50 milliliters of water was placed in each tumbler. The tumblers were sealed, and the samples tumbled for one week each.

A variety of abrasives were tested from very coarse to medium quartz sand, volcanic and carbonate (ooid) sand, and glass spheres. Glass spheres 1-2 mm in size were chosen as the 'abrasive.' These spheres had hardness similar to quartz, were equant, and did not have irregular shapes that might break off and add to the mud fraction produced. After one week of tumbling, the samples were removed from the tumbler and analyzed by both sieving and settling.

Sand samples were also examined under binocular microscope, and the mud produced by tumbling was examined under a polarizing petrographic microscope.

Both natural beach sands and sands from proposed borrow areas in Broward County were subjected to abrasion in tumbling barrels. Natural beach sands were collected from beach areas along sections of Ft. Lauderdale beaches in Broward County that had no history of renourishment and were not near sites of renourishment. Sand samples were dry sieved to determine the weight in each size fraction prior to tumbling. The sieved size fractions coarser than 125 microns were then recombined and placed in the tumbler. The 63-125 and less than 63 micron sieved fractions were not used in the abrasion study. Removing these assured that all the material found in the finer fractions following tumbling was produced through abrasion.

Borrow area sands of a variety of visible qualities were chosen. Sample BC-01-01 (6.7 ft sediment depth in proposed borrow area I) was chosen for its abundance of rounded and polished carbonate grains in the coarser sand fractions. Four other samples were chosen as typical of the proposed borrow material, having an abundance of unabraded platy, rough surfaced, or angular skeletal grains. These samples might appear acceptable beach sand through sieved grain size, but they were hypothesized to abrade or break easily, producing an large amount of suspension transported fine sand, silt and clay-sized particles during abrasion in the beach plunge/swash zone.

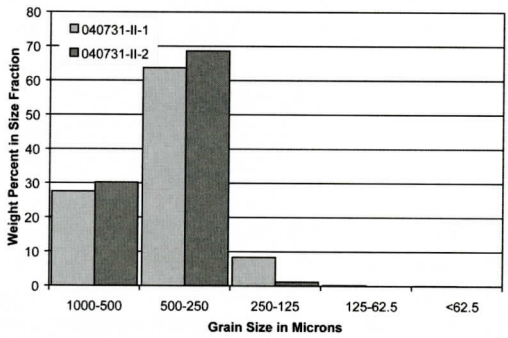

Figure 6. Sieve analysis of representative sands from the natural beaches of Ft. Lauderdale in Broward County north of Port Everglades inlet channel.

carbonate grains are cream to tan-colored, solid, robust shell fragments, sub-rounded to rounded and polished. Robust carbonate grains are mostly mollusc and Pleistocene limestone fragments.

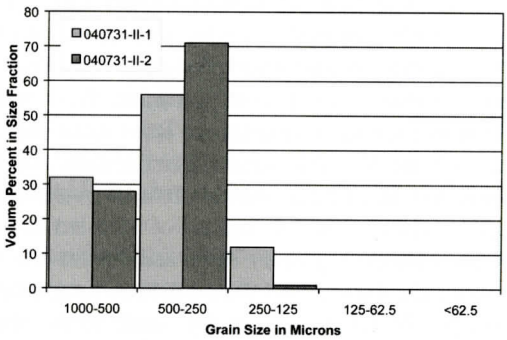

Figure 7. Settling analysis of the same representative sands from the natural beaches of Ft. Lauderdale in Broward County north of Port Everglades inlet channel.

RESULTS

Evaluation of Proposed Borrow Sands, Broward County

Grain Size and Composition

Most of the beaches north of the Port Everglades inlet channel are natural and have not received artificial beach fill. The natural beach sand is a quartz-carbonate mixture that is 90 percent between 250 and 1000 microns in size whether by sieving or settling analysis (Figures 6 and 7). No sand is finer than 125 microns. The

Forty-nine sediment samples from proposed borrow areas I, II and III (Figure 1B) were analyzed for grain size by sieving and for grain character under the microscope. The average sieved grain size distribution of the samples in each borrow area is given in Figure 8. Proposed borrow area I is nearest to shore and area III is furthest from shore. There is a progressive decrease in the percentage of sand in the 250-1000 micron fractions from the natural beach sand (Figure 6) to area I, area II and area III (Figure 8). There is also an increase in the amount of material in the less than 250 micron fractions

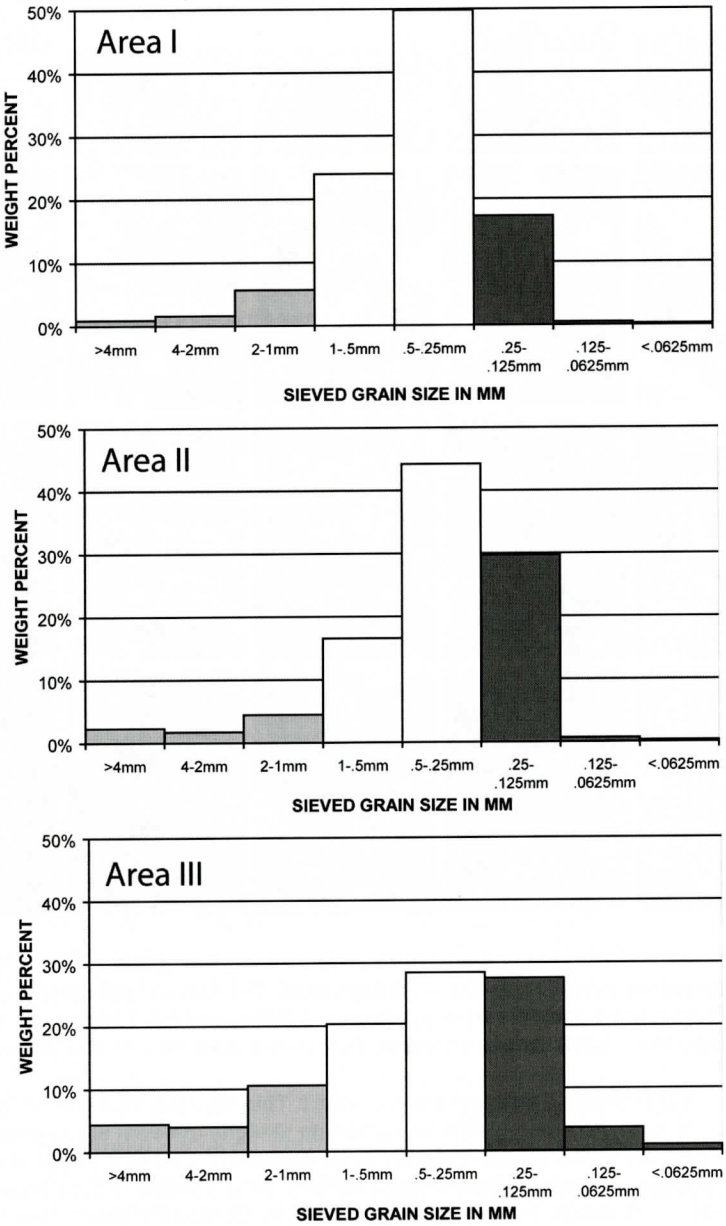

Figure 8. Average sieved grain size for samples from Broward County proposed borrow areas I, II and III. White bars are grain fractions similar to the natural beach sand sizes (1.0-0.25 mm). The coarser than one millimeter fraction (light grey) is mostly delicate, ornamented and platy shells. The dark pattern is sand finer 0.25 mm and thus unsuitable for Broward beaches.

and in the coarser than 1000 micron fractions.

At first look, this may appear as a simple dilution – an admixture of coarser and finer material to the natural beach sand component. *This is not the case.* The nature of the grains in the 500-1000 and the 250-500 micron size fractions of the proposed borrow areas are different from the grains on the natural beach. In addition, the coarser than 1000 micron fractions in the proposed borrow areas are different than the type of grains that would occur in natural beach sand.

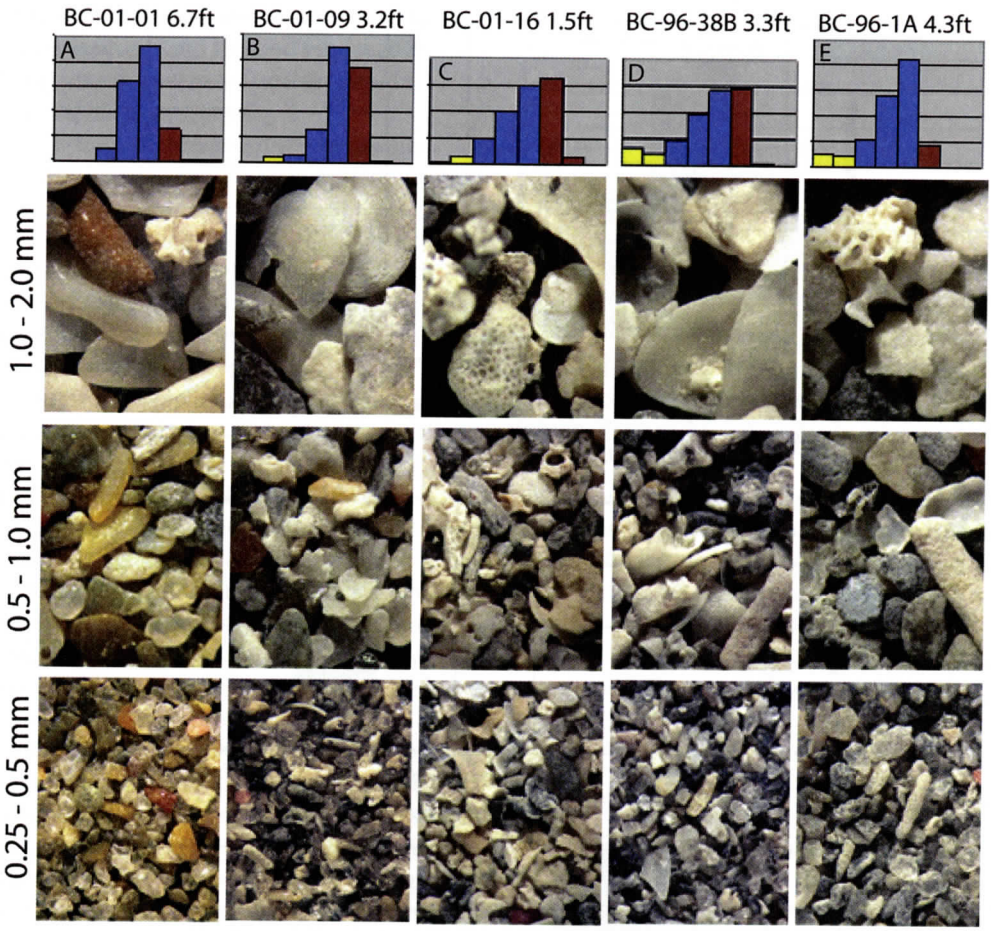

Figure 9. Samples from vibracores taken from proposed borrow areas I, II, and III. These sand samples were tested for durability in the tumbling barrel. The sieved grain size is graphed above photographs. From left: >4 and 4-2 mm are yellow; 2-1, 1-0.5, and 0.5-0.25 mm are blue; and 0.25-0.125, 0.125-0.062, and <0.062 mm is in brown. Below is a summary of characteristics for each sample.

A. Core BC-01-01 6.7 ft depth. Proposed borrow area I. This was the only one of the 49 collected samples that had robust, polished grains of carbonate skeletal material in the coarser sand fractions. About 30 percent of the carbonate grains are delicate or dull and rough surfaced. Quartz forms about 40 percent of the less-than-1-mm fractions. Nine percent is finer than 250 microns.

B. Core BC-01-09 3.2 ft depth. Proposed borrow area II. Carbonate grains are not robust but mostly platy or delicate, and many grains are rough-surfaced. Quartz forms about 30 percent of the sand, mostly in the less-than-0.5-mm fraction. Sample is 37 percent finer than 250 microns.

C. Core BC-96-16 1.5 ft depth. Proposed borrow area III. Samples from proposed borrow area III, being furthest offshore have essentially no quartz. Carbonate skeletal grains are thin and platy or delicate. Carbonate grain surfaces are either delicately ornamented or rough-surfaced. Thirty six percent is finer than 250 microns.

D. Core BC-96-38B 3.3 ft depth. Proposed borrow area II. This sample is about 30 percent quartz. Carbonate grains are either thin and platy or rough-surfaced. Many are hollow or porous inside.

E. Core BC-96-1A 4.3 ft depth. Proposed borrow area I. Sand is about 40 percent quartz, mostly finer than 500 microns. Carbonate grains are a mix of robust and delicate grains, but even the robust grains have delicate surfaces.

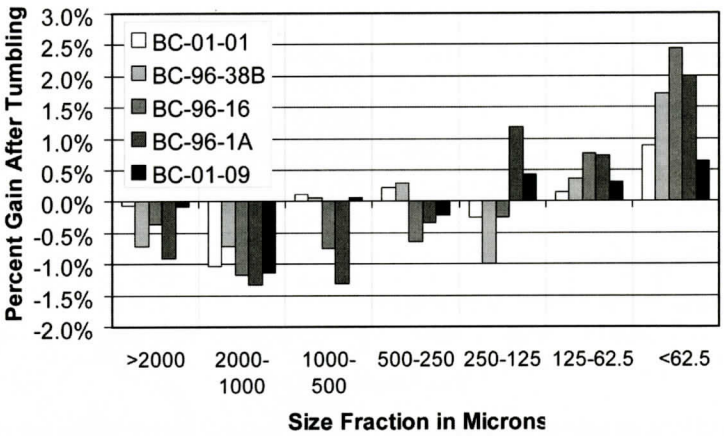

Figure 10. Graph of loss or gain of borrow area material in the different sediment size fractions following one week of tumbling. These sand samples are from vibracores collected in the proposed borrow areas I, II and III offshore Broward County and are illustrated in Figure 8A-E. The less than 125 micron size fractions were removed prior to tumbling so that all increase in these fractions is from breakage or abrasion of the coarser fractions.

Figure 9 illustrates five of the 49 samples from proposed borrow areas I, II and III. Sample BC-01-01 from 6.7 ft depth (Figure 9A) is the only one of the 49 samples that had carbonate components that were robust, rounded and polished. These beach-type grains accounted for about two thirds of the grains in the greater-than-250-micron fractions of this sample. The remaining 11 samples from proposed borrow area I had few or no robust, polished beach-derived carbonate grains. None of the samples from proposed borrow areas II and III had any robust, polished, beach-derived, carbonate grains.

Rather, the carbonate skeletal grains in 48 out of 49 of the samples are delicate platy, delicate porous, and/or rough surfaced grains. Rough-surfaced grains are those whose surface has been modified by microborings and micritization. Thin platy grains include mollusc shells and shell fragments. Thin, platy and porous grains include benthic foraminifera and *Halimeda* (a calcifying green algae). Porous grains include fragments of bryozoa, coral, foraminifera, echinoid and hollow calcifying worm tubes. Rough-surfaced grains include both delicate and robust mollusc fragments, Pleistocene limestone fragments, calcareous spicules of soft corals, and benthic foraminifera.

Quartz grains comprise about 40 percent of the less than 600-micron-sized grains in proposed borrow area I, 20-30 percent in area II, and less than 5 percent in area III.

Thus, the proposed borrow area sands are entirely different in grain character than that found in the natural beaches of Broward County. These differences are in composition (decreasing quartz grains seaward), texture (increasing fine and coarse carbonate components), nature of the carbonate grains (increased delicate, platy, and porous grains), and character of the grain surface (mostly with surface ornamentation or a rough pitted surface from microboring and micritization). The durability and transport behavior of these different borrow area sands must be questioned.

Carbonate Grain Durability

During one week of tumbling, all five samples from the proposed Broward County borrow area sands lost weight of material from the sieved size fractions coarser than 1000 microns and gained weight in the less than 125 micron fractions. The samples with carbonate grains appearing more robust, rounded and polished (BC-01-01 and BC-01-09) lost about one percent of the coarser sand to the fine fractions through abrasion (Figure 10). The samples with

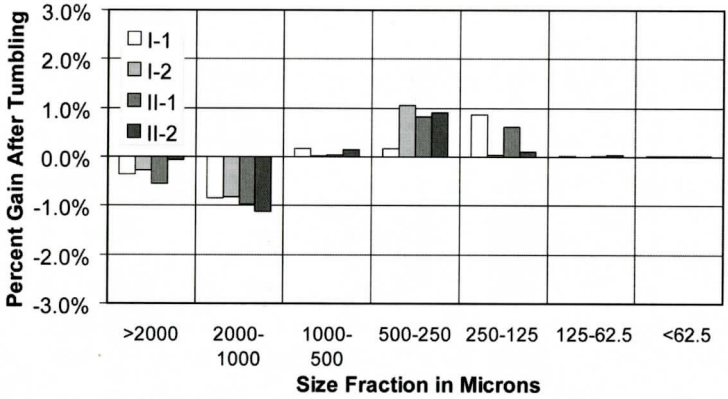

Figure 11. Graph of loss or gain of natural beach material in the different sediment size fractions following one week of tumbling. Sand samples are from natural beaches in Ft. Lauderdale, Broward County, that have not been previously renourished. The less than 125 micron size fractions were removed prior to tumbling so that all increase in these fractions is from breakage or abrasion of the coarser fractions.

grains appearing less robust, more angular and with surface ornamentation lost two to three percent of the coarser sand to the finer fractions through one week of tumbling.

Natural beach sands from Broward County beaches with no history of beach fill placement were also subjected to the same one week of tumbling with the same glass sphere abrasive. These natural beach sands produced less than 0.1 percent of particles finer than 125 microns. Rather, 1-1.5 percent of the coarser than 1mm fraction was broken to particles 125-500 microns (Figure 11).

In addition, a sample of platy mollusk shell and foraminifera tests was tumbled for one week to demonstrate how platy grains respond to abrasion. The sample fraction used was 1-2 mm (Figure 12 A). An equal weight of 250-500 micron quartz, 500-1000 micron quartz, 2000-4000 micron quartz, and 250-500 micron ooids served as abrasives in separate trials. After one week the platy grains with the very coarse sand abrasive had mostly broken into smaller size fractions, and shells had significant fresh abrasive wear on the surface (Figure 12). The trials with medium and coarse quartz and ooids resulted in a different style of breakdown – punching out the centers and breaking off the outer growth layers of the foraminifera (Figure 12). These tumbling experiments illustrate the fate of delicate and thin platy particles placed in the beach surf and swash zone. They will break and abrade down into particles finer than those which will be stable on the beach. The new finer particles will move off the beach as short- and long-term suspension load.

In laboratory tumbling barrel abrasion studies of proposed borrow area sands from the continental shelf offshore Broward County, one to three percent of the sample was abraded to particles less than 125 microns in only one week of tumbling. This was true for even the most beach-like appearing sands – those containing mostly (but not entirely) robust, rounded and polished carbonate grains.

These borrow area sands abraded to produce particles finer than 125 microns at a rate 10-30 times faster than natural beach sands subjected to the same tumbling barrel abrasion test. Abrasion of both natural beach and proposed borrow area sands resulted in breakage of some of the coarse sand particles (>1000 microns), producing particles 125-500 microns in size.

Historical Renourishment Projects in South Florida

Over the years, a variety of dredge and fill projects have been undertaken along Florida's Atlantic coast to replenish eroded beaches. Sev-

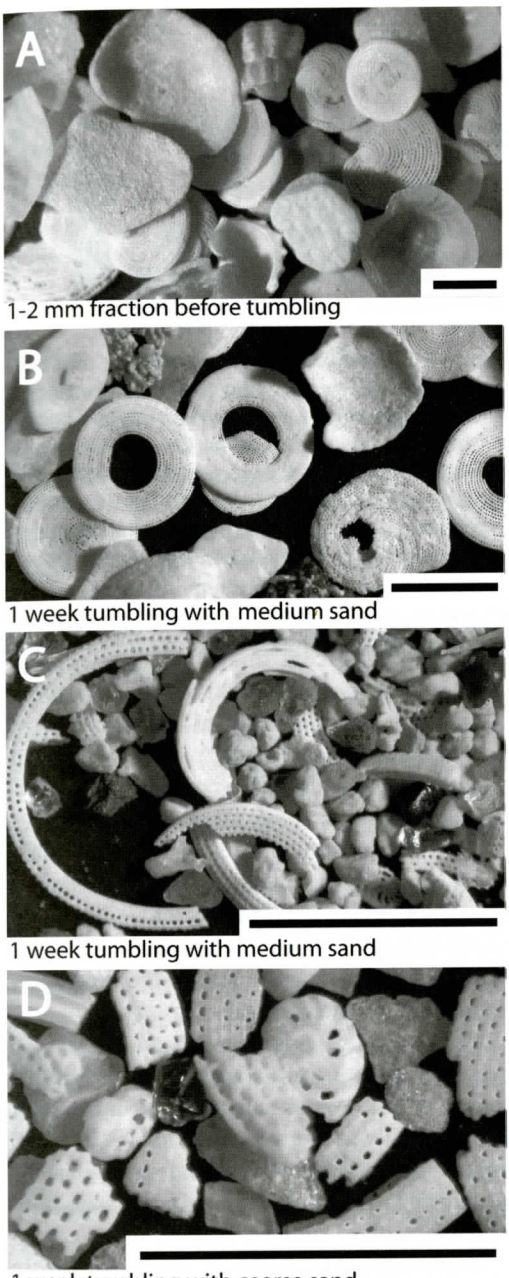

Figure 12. Tumbling of one to two millimeter thin, platy skeletal grains of shell and foraminifera. A. Sample before tumbling. B and C. After one week tumbling with medium sand, foraminifera have centers punched out and growth rings removed. D. After one week of tumbling with very coarse quartz sand, foraminifera and shell is crushed and shell shows fresh impact abrasions. Scale bars are 1 mm.

eral of these provide valuable insights as to why previous renourishment techniques have failed. Statements below are based on the senior author's observations and analyses over the past 34 years.

Miami Beach

Over a several year period around 1980, the entire length of Miami Beach was filled creating a very broad beach. The beach fill was added not because of historical erosion but because of overzealous development. The fill sand was pure skeletal carbonate derived from borrow pits well seaward on the Continental Shelf (Figure 1C).

Since the beach fill was placed, the offshore environment became very frequently turbid. Siltation and reduced light penetration has severely stressed offshore hard-bottom communities. Annual growth banding on surviving corals are much narrower (Telesnicki and Goldberg, 1995a,b). Tumbling barrel abrasion studies of the Miami Beach fill produced results similar to that described above for the Broward County proposed borrow material. In one month of tumbling, 8-10 percent of the fill sediment broke down into particles too fine to remain on the beach (Yanich and Wanless, unpublished data).

John U. Lloyd State Park

The state park is located immediately south of the south jetty of the Port Everglades Shipping Channel inlet, just south of Ft. Lauderdale (Figure 1). Because jetties block the net southward longshore drift of sediment, the shore is highly erosional. Several beach fill projects have been undertaken to offset this erosion, the most recent in 1989 and 2005. Sand was obtained from one of the offshore elongate troughs in the limestone surface. The sand was, like Miami Beach, skeletal carbonate. Mean settling grain size of one fill effort was 125 microns (authors' analyses), much too fine to remain on the beach. In addition, the sand is predominantly delicate and porous skeletal material, rapidly abrading and breaking in the surf and swash zone.

Figure 13 (top) shows the severely eroded

Figure 13. TOP—High turbidity levels off of the historically renourished beach at John U. Lloyd State Park, just south of Port Everglades Shipping Channel in Broward County. Photo taken March 6, 2004. BOTTOM.—*Acropora palmata* thrives on rocky bottom in four to five meters of water about 300 meters seaward of the Ft. Lauderdale Beach in central Broward County (north of Port Everglades Shipping Channel). The beach has never been renourished. Photo taken July 25, 2004.

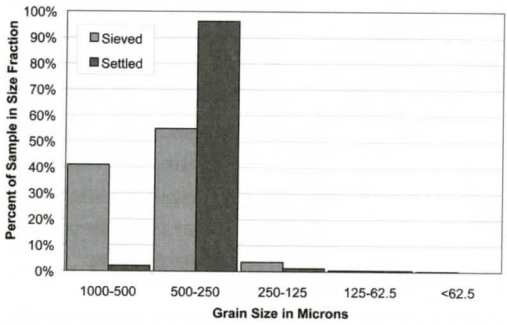

Figure 14. Comparison of the sieving and settling analysis of the less-than-1,000-micron fraction of natural beach sand from the beach at Bob Graham Park in Martin County. The sand behaves finer in settling analysis than sieving because the coarse (sieved) shell settles together with the medium grained quartz and robust shell in the 250-500 micron size fraction.

beach in 2004. The intense nearshore turbidity is the result of continued erosion and pulverization of previous beach fill materials. The once flourishing hard-bottom and coral reef communities (which occurred near the end of the jetty) are now mostly dead. To the north of Port Everglades inlet, the Ft. Lauderdale beach has never been renourished and the water was clear for snorkeling on the same day as the photo was taken. This persistently clear water permits active coral growth on the limestone bottom within 300m of the beach (Figure 13, bottom).

Martin County Beach Fill

The natural beach in Martin County (Figure 1) has tan quartz-carbonate sand that is greater than 95 percent coarser than 250 microns and less than 0.5 percent finer than 125 microns. Quartz comprises about half of the less-than-500-micron fraction. Most of the sand coarser than 500 microns is robust, rounded, polished skeletal shell material. The comparison of sieving and settling analyses (Figure 14) illustrates how the coarser sieved shell material (500-1000 micron fraction) mostly settles as though it were finer grains (250-500 microns). This natural beach sand is typical of the beach sand along the east Florida coast except in the more protected southern Miami-Dade County.

Martin County implemented an emergency beach fill project in the spring of 2005 in response to the erosion during 2004 hurricanes. Fill material was dredged from an offshore site. Figure 15 shows the sieving and settling analysis of beach fill material from a composite sample collected on April 22, 2005.

The beach fill is strikingly similar in texture and grain type to the natural beach sand – except for the addition of 6-7 percent material finer than 63 microns. This significant mud admixture will be released into the adjacent marine waters as the beach erodes, causing a long-term reduction in water clarity in the adjacent shelf waters and a moderate long-term siltation stress to the bottom communities.

The fill sand is mostly carbonate shell frag-

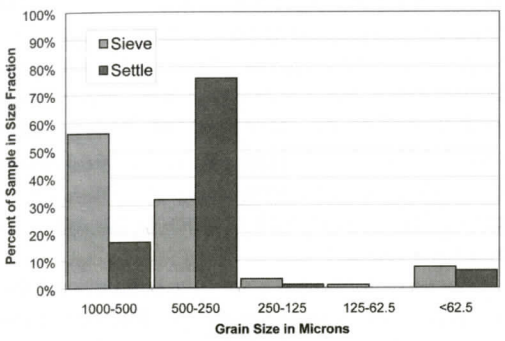

Figure 15. Textural analysis of the less-than-1,000-micron portion of offshore-derived fill placed on the beach at Bob Graham Park in Martin County in the spring of 2005. About 92 percent of the fill sample is 250-1000 microns. The striking difference with the natural beach sand is the six to seven percent of the fill sample that is less than 63 microns. Even ignoring future abrasion, every 15 cubic yards of beach fill will release one cubic yard of mud to the offshore environment.

ments with quartz varying along the beach from 10-20 percent of the less-than-500-micron fraction. Skeletal fragments in the 250-1000 micron fractions are mostly robust, rounded and polished shell fragments.

The beach fill has a large amount of mollusc shells. These are not rounded and polished but whole and ornamented. If they remain in the beach zone, they will be fragmented by storm waves and abraded in the surf and swash zone, releasing additional turbidity. These large shells were not incorporated into the textural analysis samples.

St. Lucie County Fill Project

Portions of southern St. Lucie County (Figure 1) had an emergency beach fill project following the 2004 hurricane season. The fill material was taken from an upland quarry source. On April 22, 2005 at Normandy Beach Park the recently emplaced beach material was being removed from the beach system nearly as quickly as it was placed (Figure 16 A). There was a cliff on the shore where a recent winter storm had removed the material. Seaward, the previous tan beach surface was re-exposed (Figure 16 A). Sieve and settling analysis of this

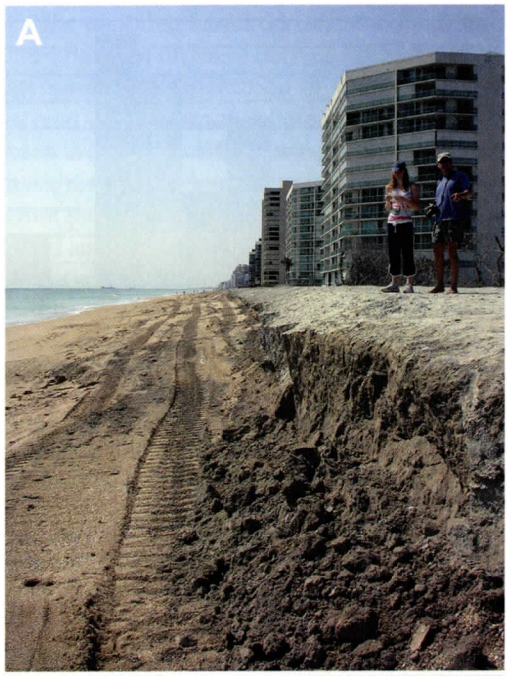

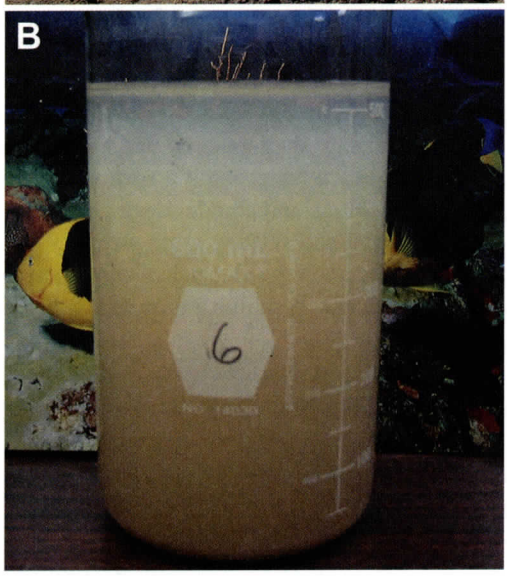

Figure 16. Top—View looking south near the north end of a beach fill project at Normandy Beach, St. Lucie County on April 22, 2005. Recent winter storms completely washed away all the new grey-colored fill reached by the waves, leaving a cliff fronting the narrow remaining fill. The tan-colored old beach is re-exposed. Bottom—Photograph following 24 hours of settling in a beaker of the sieved less-than-63-micron fraction of the fill material. This mud fraction is 10 percent of the fill material.

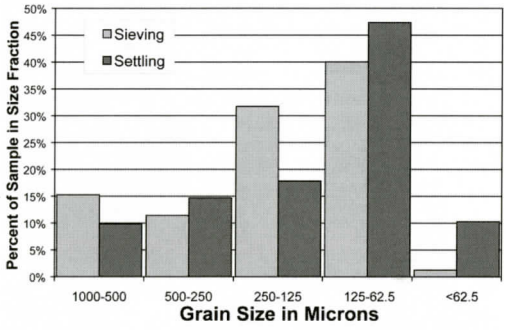

Figure 17. Comparison of sieving and settling analysis of less than one mm size fraction of fill material placed on Normandy Beach, St. Lucie County, Florida in April of 2005. Sand settles as much finer particles than indicated by sieving. The graph groups full phi size fractions.

carbonate and organic fill material both show that this material is much too fine to remain in the beach zone. In addition, the less-than-63-micron fraction has an extremely fine component that remains in suspension for days even in the quiet conditions of a beaker (Figure 16 B).

The portion of the fill sand coarser than 1 mm (23 percent by sieving or 17 percent by settling) is thin platy shell material that will not remain in the beach zone, and if a portion does, it will quickly break and abrade down.

The sieving and settling grain size analyses of the fill placed on the St. Lucie County beaches provide an excellent illustration of the different analysis techniques (Figure 17).The settled sample shows a pronounced shift to the finer sizes as compared to sieving. The skeletal carbonate sands behave as much finer grains than is indicated by the sieve analysis. This is to be expected as the skeletal grains in this fill are thin and platy or porous. (Again, the settling tube is calibrated with respect to equant subrounded quartz.)

A closer look at the settling behavior of the fill placed on Normandy Beach illustrates how completely unsuitable this material was for beach renourishment (Figure 18). Natural beach sand in the area is 98 percent coarser than 250 microns, similar to that illustrated in Figure 16 for Martin County. Recall that with higher energy, grains even coarser than 200 microns will move in suspension. That is clearly the case for Martin and St. Lucie Counties that where there is an abrupt cutoff in size distribution at or just coarser than 250 microns. Only 24 percent of this fill was coarser than 250 microns, and nearly all of that was too delicate or porous to remain on the beach. (This fill was completely eroded from the beach in Figure 16 A.)

About 68 percent of the material moves in short-term suspension (40-250 microns). This material is presently being dispersed across the adjacent shelf, smothering benthic communities. As this fine sand and silt material is so abundant and is mostly too fine to remain on the

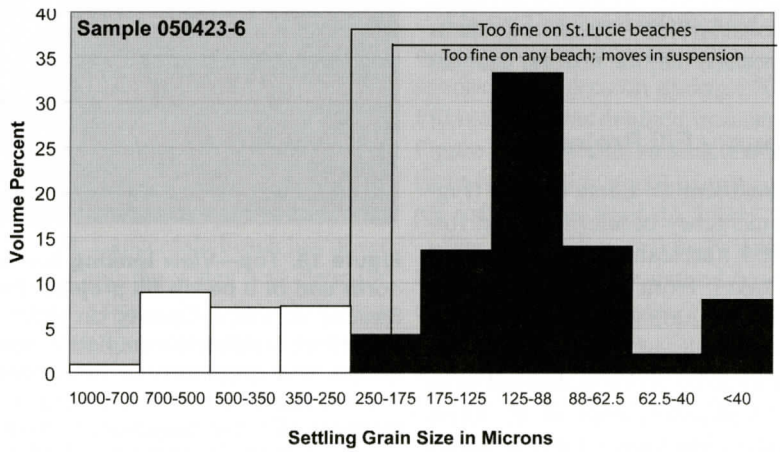

Figure 18. Settling grain size analysis shown in ½ phi intervals for material placed on Normandy Beach, St. Lucie County in April, 2005. Over 75 percent of the material is too fine to remain in the beach zone.

shelf, it will move around the shelf rapidly smothering different areas for years to come until it moves to a stable, low energy site. Finally, eight percent of the fill is finer than 40 microns and will move in long-term suspension. This will produce persistent lowering of water clarity across the adjacent shelf for years. The tan color and the presence of roots, suggests that this fine material was a soil.

DISCUSSION

The valuable benthic, sandy, hardbottom, and coral reef habitats adjacent to these beaches cannot handle the environmental degradation of the intensifying beach 'renourishment' activity using current practices. Beach fill projects along southeast Florida both are not working, resulting in economic waste (Pearson and Riggs, 1981), and are severely degrading the adjacent marine environment. This failure is resulting from a combination of five causes. First, suitable inexpensive sand is increasingly difficult to find nearby, yet local sediment sources are still being used. Second, criteria used for evaluation of silicic-clastic (quartz) sands are being directly applied to sediments composed of skeletal carbonate sand. Third, established understanding of sediment dynamics in the beach system is not being utilized in the selection of sands for renourishment. Fourth, too much fine, suspension-transported sand is permitted as 'overfill' in beach fill projects. Fifth, biologic monitoring studies are inadequate and rarely applied to mitigation attempts (Peterson and Bishop, 2005).

Sand used in recent south Florida beach renourishment projects is not acceptable for a beach setting. Much of the sand is too fine when grain size is evaluated with a sieve, and even larger portions of the samples are unsuitable when evaluated by settling analysis. Further, the suitable sand sizes are dominated by delicate, angular, porous carbonate skeletal grains that will quickly fragment and abrade in the beach zone, producing large volumes of fine-grained sand to mud. This fine material will move offshore in suspension and not stay in the beach zone.

The tumbling barrel documentation of rapid breakdown of offshore-derived skeletal carbonate sands is a verification of what can be observed on any beach where such sands have been used as beach fill. Such beach fill projects have resulted in long term increased turbidity (fine particulates suspended in the water column) and bottom siltation (from suspended fine sands and muds moving offshore).

The current criteria and permit approval for beach renourishment sands allow excessive amounts of suspension-transported sand and do not adequately address particle durability or hydrodynamic behavior. Criteria must be revised and rigorously enforced to eliminate use of material that will move off the beach in suspension and must require adequate evaluation methods such as the settling tube analysis and durability testing. The problems being encountered in southeastern Florida should have direct application to tropical beaches throughout the world.

ACKNOWLEDGEMENTS

Data analysis and evaluation was conducted at the University of Miami sedimentology lab on the Coral Gables Campus. Logistical support from Dan and Stephanie Clark facilitated the sampling process. Susan Ebbs, Dan and Stephanie Clark and Stephen Attis served as diving partners and guides to the Broward County offshore area. Thanks to Yohan Yanich for his laboratory assistance in analyzing the Miami Beach renourishment sands. Research was conducted with the aid of a Summer Scholar research award from the College of Arts and Sciences, University of Miami. Ken Lindeman generously offered technical support and suggestions for improving the manuscript.

REFERENCES CITED

Bagnold, R.A., 1966, An approach to the sediment transport problem from general physics: U.S. Geological Survey Professional Paper 442-I.

Blott, S.J. and Pye, K., 2004, Morphological and sedimentological changes on an artificially nourished beach, Lincolnshire, U.K.: Journal Coastal Research, v. 20, p. 214-233.

Braithwaithe, C.J.R., 1973, Settling behavior related to sieve analysis of skeletal sands: Sedimentology v. 20,

p. 251-262.

Bush, D. M., Neal, W. J., Longo, N. J., Lindeman, K. C., Pilkey, D. F., Esteves, L. S., Congleton, J. D., and Pilkey, O. H., 2004. Living with Florida's Atlantic Beaches: Coastal Hazards from Amelia Island to Key West. Durham, NC: Duke University Press, 310 p.

Davidson, A.T., Nicholls R.J., Leatherman S.P., 1992, Beach nourishment as a coastal management tool: an annotated bibliography on developments associated with the artificial nourishment of beaches: Journal Coastal Research v. 8, p. 984-1022.

Galvin, C., 1990, Importance of longshore transport. Shore and Beach v. 58, p. 31-32.

Hackney, C.T., Posey M.H., Ross S.W., Norris A.R., 1996, A review and synthesis of data on surf zone fishes and invertebrates in the South Atlantic Bight and the potential impacts from beach renourishment: US Army Corps of Engineers, Wilmington.

Hughes, T. and Connell J. 1999, Multiple stresses on coral reefs, a long-term perspective: Limnology and Oceanography, v. 44, p. 932-940.

Kobluk D., 1977, Calcification of filaments of boring and cavity-dwelling algae, and the construction of micrite envelopes, *in* Romans R.C. (ed) Geobotany. Plenum Publishing, New York.

Lindeman K. and Snyder, K., 1999, Nearshore hardbottom fishes of southeast Florida and effects of habitat burial caused by dredging: Fishery Bulletin-NOAA 97L, p. 508-525.

McCave, I.N., 1970, Sand waves in the North Sea off the coast of Holland: Marine Geology v. 10, p. 199-255.

Nelson, W.G., 1989, Beach nourishment and hardbottom habitats: the case for caution: Proc. 1989 National Conference Beach Preservation Technology, p. 109-116.

Newman, D.E., 1976, Beach replenishment: sea defenses and a review of the role of artificial beach replenishment: Proceedings Institution Civil Engineers, v. 60, p. 445-460.

Nordstrom, K.F., 2000, Beaches and Dunes of Developed Coasts: Cambridge University Press, Cambridge.

Passega, R., Rizzini, A. and Borghetti, G., 1967, Transport of sediments by waves Adriatic coast shelf, Italy: American Association Petroleum Geologists Bulletin, v. 51, p. 1304-1319.

Pearson, D.R. and Riggs, S.R., 1981, Relationship of surface sediments on the lower forebeach and nearshore shelf to beach nourishment at Wrightsville Beach, North Carolina: Shore and Beach, v. 49, p. 26-31.

Peterson, C.H. and Bishop M.J., 2005, Assessing the environmental impacts of beach nourishment: BioScience, v. 55, p. 887-896.

Peterson, C.H., Hickerson, D. and Johnson, G., 2000, Short-term consequences of nourishment and bulldozing on the dominant large invertebrates of a sandy beach: Journal Coastal Research, v. 16, p. 368-378.

Pilkey, O.H., 1983, The eroding shores and the disappearing beach: Geophysics, v. 2, p. 50-53.

Riddell, K.J. and Young, S.W., 1992, The management and creation of beaches for coastal defense: Journal Inst. of Water Environment Management, v. 6, p. 588-597.

Sengupta, S. and Veenstra, H.J., 1968, The behavior of large particles falling in quiescent liquids: Sedimentology, v. 11, p. 83-98.

Subcommittee on Sedimentation Inter-Agency Committee on Water Resources, 1957, A study of methods used in measurement and analysis of sediment loads in streams: report No. 11 The development and calibration of the Visual-Accumulation Tube: St. Anthony Falls Hydraulic Laboratory, Minneapolis.

Telesnicki, G.J. and Goldberg, W.M., 1995a, Effects of turbidity on the photosynthesis and respiration of two south Florida reef coral species: Bulletin Marine Science, v. 57, p. 527-539.

Telesnicki, G.J. and Goldberg, W.M., 1995b, Comparison of turbidity measurement by transmissometry and its relevance to water quality standards: Bulletin Marine Science, v. 57, p. 540-547.

United States Army Corps of Engineers, 2004, Maps of Broward County Offshore Borrow Areas: U.S. Army Corps Engineers, Jacksonville.

Wanless, H.R. Burton, E.A. and Dravis, J., 1981, Hydrodynamics of carbonate fecal pellets: Journal Sedimentary Petrology, v. 51, p. 27-36.

Wanless, H.R., Parkinson, R. and Tedesco, L.P., 1994, Sea level control on stability of Everglades wetlands. In: Proceedings of Everglades Modeling Symposium, p. 199-223.

Wilber, P. and Stern, M., 1992, A re-examination of infaunal studies that accompany beach nourishment projects: Proceedings 1992 National Conference Beach Preservation Technology, p. 242-256.

Zeigler, J.M. and Gill, B., 1959, Tables and Graphs for the Settling Velocity of Quartz in Water, Above the Range of Stokes' Law: Woods Hole Oceanographic Institution, Woods Hole.

Zhang, K., Douglas, B.C. and Leatherman, S.P., 1997, East Coast storm surges provide unique climate record: EOS, v. 78, p. 395–397.

Zhang, K., Douglas, B.C. and Leatherman, S.P., 2000, Twentieth-century storm activity along the U.S. east coast: Climate, v. 13, p. 1748-1761.

SOUTHEASTERN GEOLOGY
V. 45, No.1, June 2007, p. 43-49

MAASTRICHTIAN (CRETACEOUS) REGULAR ECHINOIDS FROM THE ROCKEY POINT MEMBER, PEEDEE FORMATION SOUTHEASTERN NORTH CAROLINA

CHARLES N. CIAMPAGLIO

Department of Geology
Wright State University – Lake Campus
7600 State Route 703
Celina, OH 45822

PATRICIA G. WEAVER

Geology/Paleontology
North Carolina Museum of Natural Sciences
11 West Jones Street
Raleigh, NC 27601-1029
<trish.weaver@ncmail.net>

ABSTRACT

Two phymosomatoid echinoids, *Phymotaxis tournoueri* (Cotteau, 1866) and phymosomatoid ident., are described for the first time from Maastrichtian age rocks of southeastern North Carolina.

INTRODUCTION

Though Late Cretaceous and Paleogene echinoids are commonly found in quarries in southeastern North Carolina, published reports on them have been sparse. Emmons (1858), provided some of the earliest descriptions of echinoderms, mostly Eocene and younger, from eastern North Carolina. Cooke (1953) reported on Late Cretaceous irregular echinoids, including *Hardouinia* from the Peedee Formation. Kier (1980, 1997), described regular echinoids of the genera *Phyllacanthus* and *Coelopleurus*, and irregular echinoids, including *Linthia*, *Echinolampas*, *Rhyncholampas, Echinocaymus*, *Periarchus* and *Protoscutella* from the Eocene Castle Hayne Formation, as well as *Psammechinus*, *Clypeaster*, *Agassizia, Maretia* and others from the Oligocene River Bend Formation of southeastern North Carolina. Carter et al (1988), in their guide to fossil collecting in North Carolina, included figures of the Cretaceous irregular echinoid *Hardouinia mortonis*, along with Eocene echinoids *Echinolampas appendiculata,* and *Periarchus lyelli*. While local collectors have reported occurrences of Late Cretaceous regular echinoids, to date we have found no mention of Cretaceous regular echinoids from North Carolina in the literature.

Recent donations to the North Carolina Museum of Natural Sciences have brought to light two phymosomatoid echinoids, described here as *Phymotaxis tournoueri* and phymsomatoid ident. from the Rocky Point Member of the Peedee Formation. These new specimens give a more complete list of the Cretaceous echinoid fauna of southeastern North Carolina.

GEOLOGIC SETTING

The Late Cretaceous Peedee Formation is exposed in a broad, north-to-south trending belt, and it outcrops along all the major coastal plain streams from Contentnea Creek in North Carolina (Figure 1) to the Pee Dee river basin in South Carolina. Although lower portions of the formation are exposed along the northern rivers, only along the Cape Fear and Pee Dee rivers (Sohl and Owens, 1987) are both the upper and lower portions visible together. The base of the Peedee Formation rests unconformably upon the Donoho Creek Formation and is disconformably overlain by the Eocene Castle Hayne Limestone or post-Eocene sands and gravels (Harris, 1978). Reworked phosphatic pebbles and cobbles, internal molds of mol-

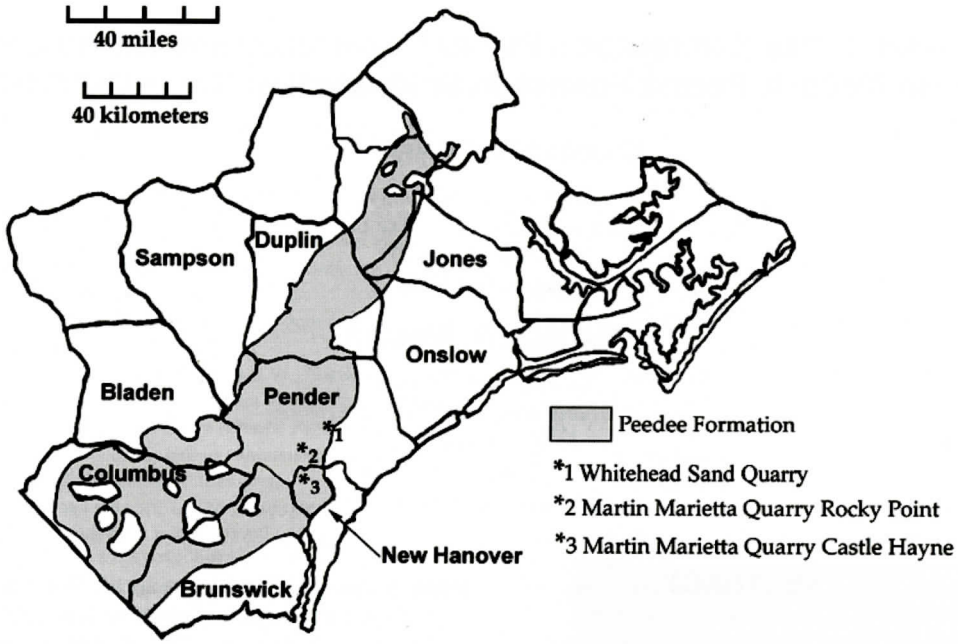

FIGURE 1 - Studied area in southeastern North Carolina, with Martin Marietta and Whitehead Sand quarries in Pender County, and Martin Marietta quarry in New Hanover County indicated. The shaded region indicates the geographical extent of the Peedee Formation. Adapted from North Carolina Geological Survey, 1994

lusks, and vertebrate material from the underlying Donoho Creek Formation are typically incorporated into basal portions of the Peedee Formation.

Lithologically, the Peedee Formation is dominated by a dark-greenish to gray, sparingly micaceous and glauconitic, argillaceous massive sand. Calcareous cemented concretions occur sporadically and, in some cases, form distinct bedding. Dark marine clays, ranging in some areas up to two meters in thickness, can be locally abundant. Calcareous sandstone ledges interbedded with firm, non-cemented sands occur at many stratigraphic levels within the formation. Additionally, sandy biomicrudite occurs near the top of the Peedee Formation along the Cape Fear River and in the Castle Hayne area, Pender County, NC (Dockal *et al.*, 1998; Sohl and Owens, 1987; Harris, 1978).

Swift (1964) divided the Peedee into two depositional units: an inner shelf unit composed of sand and muddy sand, representing the lower portion of the Peedee, and an outer shelf unit composed mainly of calcareous muddy sand and sandy mud, which represents the upper portion of the Peedee. Swift (1964) also recognized several lenses of biomicrite and biomicrudite. Hodge (1841) recognized a distinctive carbonate unit at the top of Peedee, but it was well over 100 years before the predominantly calcareous unit, the Rocky Point Member, was formally named and mapped (Swift and Heron, 1969; Wheeler and Curran, 1974; Harris 1978).

The Rocky Point Member occurs north of the Cape Fear Arch in eastern Brunswick County, most of New Hanover County, eastern Pender County, and southern Onslow County. Based upon lithological differences, Harris (1978) divided this member into four distinct lithofacies: quartz arenite; sandy, pelecypod biosparrudite; sandy, pelecypod biosparite; and sandy biosparite. The quartz arenite facies occurs at the base of the Rocky Point Member and represents a gradational change from the underlying, typical Peedee lithology to an almost pure quartz sand that is depleted of clay minerals. The quartz arenite lithofacies within the Rocky Point Member can be massive, or contain pock-

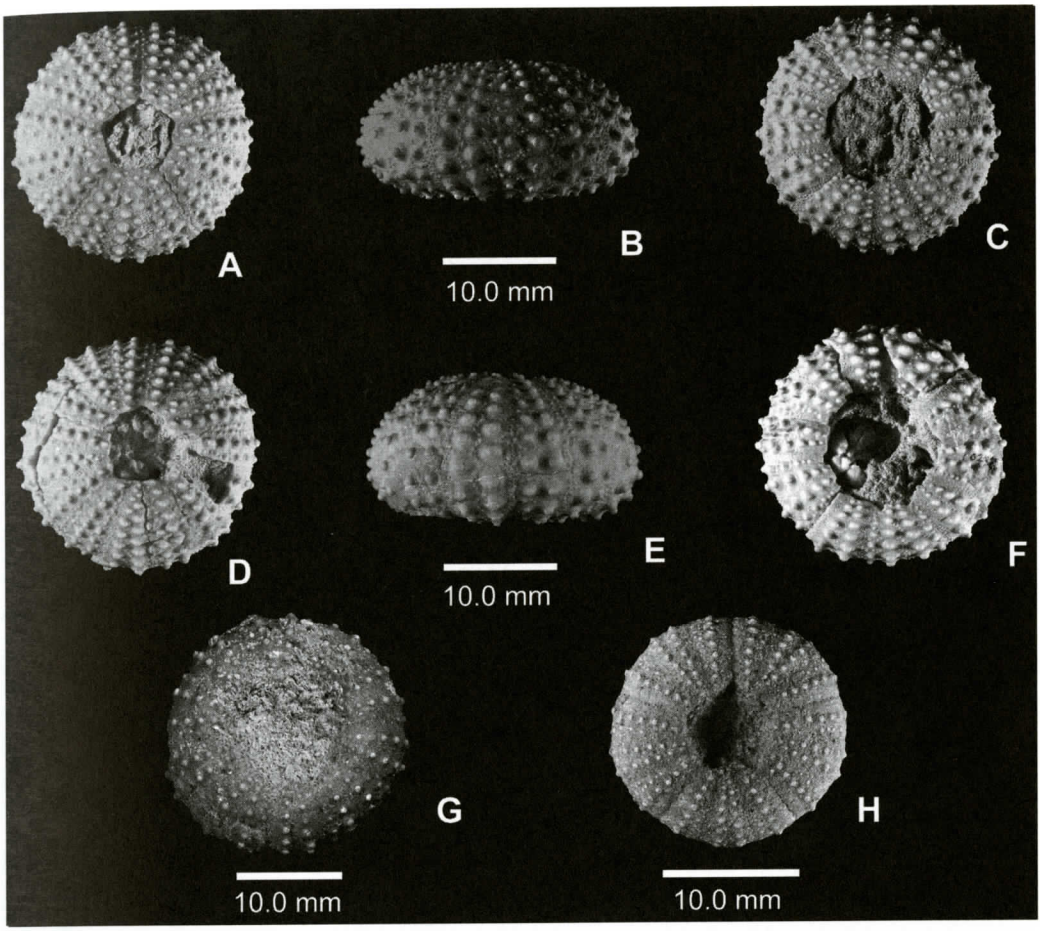

FIGURE 2 – *Phymotaxis tournoueri* (Cotteau): A-G. A, B, C, NCSM 10315 aboral, lateral, and oral view. D, E, F, NCSM 10248 aboral, lateral, and oral view. G, NCSM 10238 aboral view. Phymosomatoid genus indet. H, NCSM 10018 oral view.

ets consisting of intramicrite, intramicrudite, or biomicrudite (Harris, 1978; Sohl and Owens, 1987).

Although exposures of the quartz arenite lithofacies are restricted, it does form a large proportion of the Rocky Point Member, and is locally abundant, for example in quarries in eastern Pender County and New Hanover County. Fossils, although not common, do occur in high abundance within pockets. The macrofossil fauna includes the irregular echinoids *Hardouinia mortonis*, *H. kellumi*, an undescribed regular urchin, and both calcitic and aragonitic pelecypods including *Flemingostrea subspatulata* and *Cucullea* sp., moulds of gastropods, and occasional vertebrate material (Harris,1978; Sohl and Owens, 1987).

While there is agreement that the Peedee Formation is Maastrichtian in age (Harris, 1976, 1978; Sohl and Owens, 1991; Gohn, 1992; Wingard, 1993), the exact placement of the formation within the Maastrichtian is less certain. Gohn (1992), interpreted the lower portion of the Peedee as late Early Maastrichtian and the remainder as belonging to the middle and probably Late Maastrichtian, based on nannofossils. Alternately, based on planktonic foraminifera, Gohn determined a middle Maastrichtian age for the Peedee. Wingard (1993), based upon crassatellid bivalves determined a middle to Late Maastrichtian age for the Peedee Formation. Using molluscan biozo-

nation, the Peedee Formation correlates to the Ripley Formation and Providence Sand in Georgia and eastern Alabama, and to the upper part of the Ripley Formation and Prairie Bluff Chalk in central to western Alabama, thus placing the Peedee in the Navarroan (= Maastrichtian) Stage (Sohl and Owens, 1987; Prowell, 1994).

SYSTEMATIC PALEONTOLOGY

All illustrated specimens are housed at the North Carolina Museum of Natural Sciences (NCSM), Raleigh, North Carolina.

Superorder ECHINACEA Claus, 1876

Order PHYMOSOMATOIDA Mortensen, 1904

Family PHYMOSOMATIDAE Pomel, 1883

Genus *PHYMOTAXIS* Lambert and Thiéry, 1914

Phymotaxis tournoueri (Cotteau, 1866)

(Figure 2. A-F, H, Figure 3. A-C, Figure 4. A&B)

Diagnosis.—Test low, circular, slightly convex apically, medium-sized. Apical system not preserved. Apical scar pentagonal. Peristome circular, approximately 40 percent of diameter of test, showing buccal notches. Ambulacral plates compound, pore zones uniserial, weak phyllode development below ambitus. Tubercles imperforate, weak traces of crenulations. In ambulacral zones tubercles in rows of two. In interambulacral zones, primary tubercles in rows of four. Plates become somewhat granulate at ambitus.

Description.— Test medium, diameter at ambitus ranging in size from 38 to 44 mm. Height is less than 50 percent of diameter at ambitus. The apical system is not preserved, but leaves a somewhat pentagonal scar, ~33 percent of total width, in the better preserved specimens. Ambulacral plates show phymosomatid compounding (Figures 3A, 4A). Peristome is circular, slightly sunken, about 40 percent of the test diameter and in the better preserved specimens, NCSM 10315 and 10248, with obivious buccal notches. Where visible, pore pairs are uniserial, in arcs, becoming slightly more numerous just above the peristome. Tubercles are imperforate and where visible in NCSM 10315 and NCSM 10248 show traces of crenulations. Crenulations are not preserved in NCSM 10018 and NCSM 10220 as these specimens are not as well preserved and seem to be somewhat re-crystallized. Granules are visible near ambitus in the better preserved specimens. On ambulacral plates tubercles are in rows of two on pairs of plates (Figures 3A, 4A), smaller apically and below ambitus. On interambulacral plates tubercles form rows of four on pairs of plates (Figures 3A, 4B). Aristole's lantern, with keeled teeth, is preserved only on NCSM 10248 (Figure 3B). Spines preserved on NCSM 10220 show weak striations and a weak collar (Figure 3C).

Material.— NCSM 10315, NCSM 10248, NCSM 10220, NCSM 10018

Measurements. —

Specimen number	Height	Diameter at ambitus	Diameter of peristome	Diameter of apical scar
NCSM 10315	19.23	38.41	17.06	11.29
NCSM 10248	19.91	38.32	17.46	12.55
NCSM 10220	19.92	41.41	17.63	not preserved
NCSM 10018	21.86	44.72	19.72	not preserved

Occurrence.— Rocky Point Member of the Pee Dee Formation, Maastrichtian, Cretaceous, southeastern North Carolina. NCSM10315 and NCSM 10248 Whitehead Sand Pit, Pender County, North Carolina. NCSM 10018 and NCSM 10220 Martin Marietta Quarry near Castle Hayne, New Hanover County, North Carolina.

Discussion.— North Carolina specimens are most similar to material of *Phymotaxis*

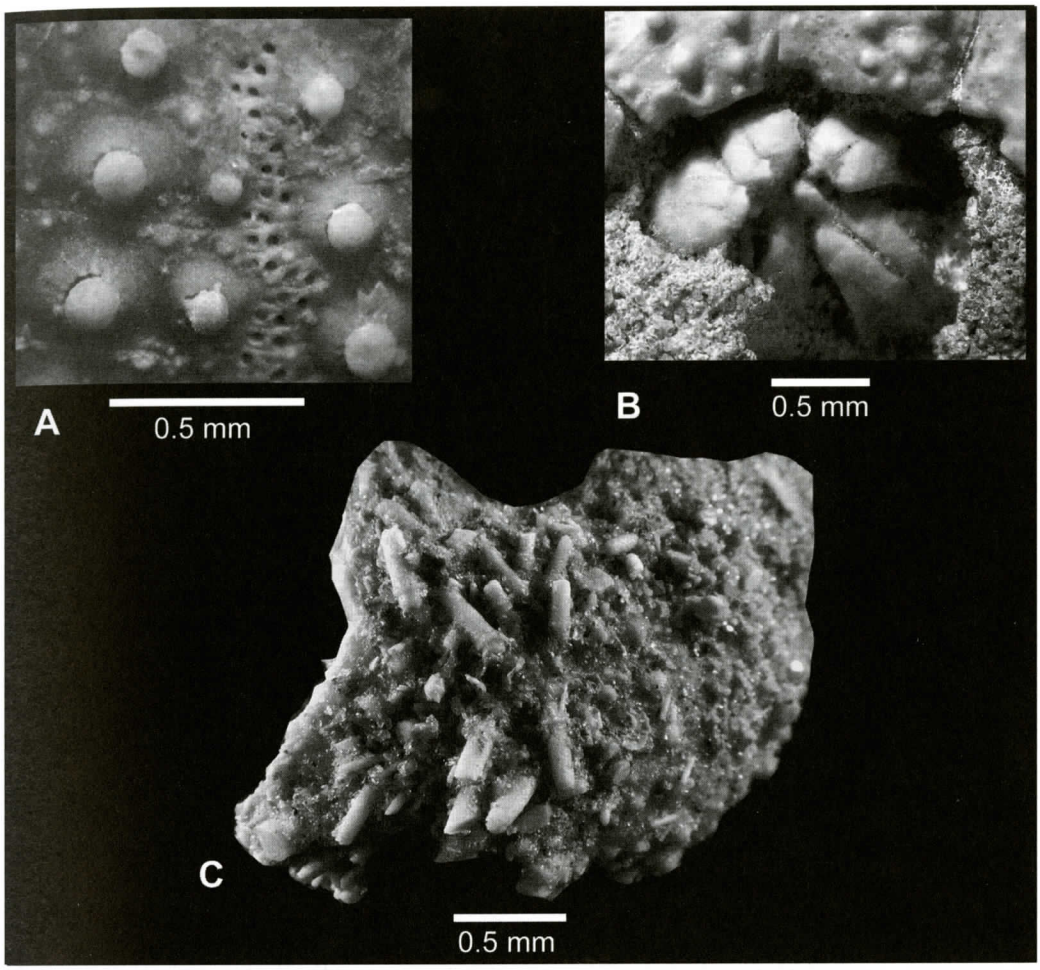

FIGURE 3 – *Phymotaxis tournoueri* (Cotteau). A, NCSM 10315 close-up view of plate morphology and pore pairs. B, NCSM 10248 detailed view of lantern. C, NSCM 10220 detailed view of spines.

tournoueri found in Europe as described by Smith and Jeffery (2000). Age, size, tuberculation and arrangement of pores in simple arcs are comparable. These specimens differ from the *Phymotaxis fifei* (Wagner, 1972) from the Late Paleocene of California in that *Phymotaxis fifei* has more pore pairs, eight to ten, per compound plate where as *Phymotaxis tournoueri has five to six*. Smith and Jeffery (2000) noted that *Phymotaxis tournoueri* differs from most species of *Phymosoma* in that the pore pairs of *Phymotaxis tournoueri* are not biserial and tubercles show only weak crenulation. Though this is the first reported occurrence of *Phymotaxis tournoueri* in North Carolina it is not unexpected. Ciampaglio and Weaver (2004) reported three, mostly European, (*Amphorometra parva*, *Hertha plana*, *Glenotremites carentonensis*) species of comatulid crinoid from the Eocene Castle Hayne Formation in southeastern North Carolina and noted they might have been re-worked from underlying Cretaceous Peedee sediments. Also, Smith and Jeffery (2000) synonomized *Rachiosoma hondoensis* Cooke 1953 from Texas with *Phymotaxis tournoueri*. More regular echinoid material from the southeastern United States needs to be studied before any coments can be made about what the significance of finding primarily European species in North America is. However, this does indicate a Tethyan influence.

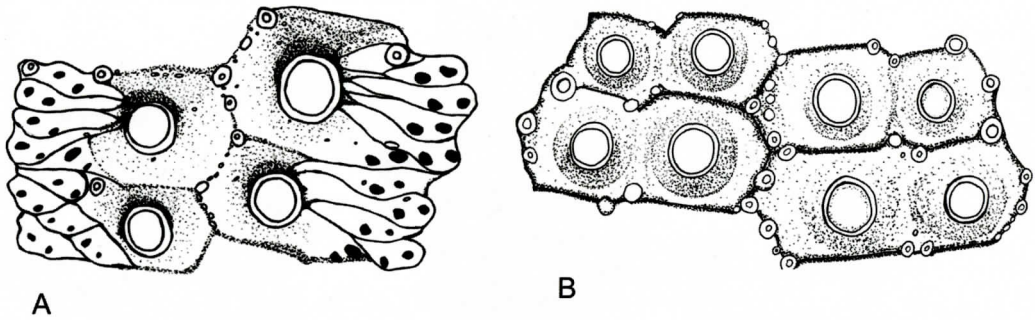

FIGURE 4 - *Phymotaxis tournoueri* (Cotteau). A, ambulacrum. B, interambulacrum.

Order PHYMOSOMATOIDA Mortensen, 1904

Genus indet.

(Figure 2.G)

Diagnosis.— Test recrystallized, low, circular, slightly convex apically, medium size. Apical system not preserved. Apical scar pentagonal. Peristome circular, approximately 38 percent of diameter of test, showing buccal notches. Tubercles imperforate. In ambulacral zones tubercles in rows of two. In interambulacral zones, primary tubercles in rows of two above ambitus, in rows of four below ambitus. Pore pairs not preserved.

Description.— Test recrystallized, medium, diameter at ambitus 38.4mm. Height is about 38 percent of diameter at ambitus. The apical system is not preserved, but leaves a somewhat pentagonal scar, approximately 33 percent of total width. Peristome is circular, slightly sunken, about 38 percent of the test diameter and shows traces of buccal notches. Pore pairs obscured by recrystallization of test. Tubercles are imperforate, and somewhat worn. On ambulacral zones tubercles are in rows of two, smaller apically. On interambulacral zones tubercles form rows of two apically and rows of four below ambitus.

Material.— One recrystallized, but fairly complete specimen, NCSM 10238.

Measurements.— Height: 12.85 mm, width: 33.38 mm, diameter of peristome:12.37 mm, diameter of apical scar: 11.13 mm.

Occurrence.— Rocky Point Member of the Pee Dee Formation, Maastrichtian, Cretaceous, Southeastern North Carolina. Martin Marietta Quarry near Rocky Point, Pender County, North Carolina.

Discussion.--- Specimen NCSM 10238 is somewhat smaller than other specimens described here. The tuberculation on this specimen is somewhat different from those described as *Phymotaxis tournoueri*. This specimen has tubercles in rows of two in the ambulacral zones and in the interambulacral zones, apically, tubercles in rows of two and rows of four below ambitus , whereas specimens of *P. tournoueri* have interambulacral tubercles in rows of four throughout. Because this specimen has been recrystallized and the plate compounding and pore arrangements are obscured, no designation below order is possible.

ACKNOWLEDGMENTS

We are extremely grateful to Rebecca Hyne, Bernie Peterson and Vic Wright for donating specimens to this study. We are also thankful to Janet Edgerton for bibliographic assistance and to Richard Chandler for photographic assistance. We are indebted to Dr. William Harris for commentary regarding North Carolina stratigraphy, also to Dr. Andrew Smith for invaluable insights regarding echinoid taxonomy, and to Burt Carter and George Phillips for their welcomed comments and review.

REFERENCES

Carter, J.G., Gallagher, P.E., Valone, R.E and Rossbach, T.J, with contributions by Gensell, P.G., Wheeler, W.H., and Whitman, D., 1988, Fossil Collecting in North Carolina: North Carolina, Department of Natural Resources and Community Development, Division of Land Resources: Geological Survey Section, Bulletin 89, 89 p.

Claus, C.F.W., 1876, Grundzüge der Zoologie. N.G. Elwert, Marburg and Lepipzig. 3rd edition , 1254 p.

Ciampaglio, C.N., Weaver, P.G., 2004, Comatulid crinoids from the Castle Hayne Limestone (Eocene), southeastern North Carolina: Southeastern Geology, v. 42, no. 3, p.179-187.

Cooke, C.W., 1953, American Upper Cretaceous Echinoidea: A shorter contribution to general geology: U.S. Geological Survey Professional Paper 254-A, 44 p.

Cotteau, G., 1866, Échinides nouveaux ou peu connus: Revue et Magazin de Zoologie, Series 2, v. 18, p. 201-209.

Dockal, J.A., Harris, W. B., and Laws, R. A., 1998, Late Maastrichtian sediments on the north flank of the Cape Fear Arch, North Carolina: Southeastern Geology, v. 37 issue 3, p. 149-159.

Emmons, E., 1858, Agriculture of the eastern counties together with descriptions of the fossils of the marl beds: Report of the North Carolina Geological Survey, 314 p.

Gohn, G.S., 1992, Revised nomenclature, definitions, and correlations for the Cretaceous formations in USGS-Clubhouse Crossroads #1, Dorchester County, South Carolina: U.S. Geological Survey Professional Paper, 1581, 39 p.

Harris, W. B., 1976, Rb-Sr glauconite isochron, Maestrichtian unit of Peedee Formation (upper Cretaceous), North Carolina: Geology (Boulder), v. 4 issue 12, p. 761-762.

Harris, W. B., 1978, Stratigraphic and structural framework of the Rocky Point Member of the Cretaceous Peedee Formation, North Carolina: Southeastern Geology, v. 19 issue 4, p. 207-229.

Hodge, J.T., 1841, Observations on the Secondary and Tertiary formations of the southern Atlantic States: New Haven, CT : Kline Geology Laboratory, v. 41, no. 2. p. 332-344.

Kier, P.M., 1980, The echinoids of the Middle Eocene Warley Hill Formation, Santee Limestone, and Castle Hayne Limestone of North and South Carolina: Smithsonian Contributions to Paleobiology, no. 39, 102 p.

Kier, P.M., 1997, Oligocene echinoids of North Carolina: Smithsonian Contributions to Paleobiology, no. 83, 37 p.

Lambert, J., and Thiéry, P., 1914, Essai de nomenclature raisonnée des échinides: Librairie Septime Ferrière, Chaumont, 607 p.

Mortensen, T., 1904, The Danish expedition to Siam, 1899-1900: II Echinoidea (1): [K.] Danske Videnskabernes Selskabs, Matematiska-Fysiske, Skrifter, Köbenhavn, series 7, v.1, p. 1-24.

Pomel, A., 1883, Classification méthodique et genera des échinides vivants et fossils: Adolf Jourdan, Alger, 131 p.

Prowell, D.C., 1994, Late Cretaceous stratigraphy in the central coastal plain of South Carolina; new evidence from drill holes near Lake Marion, Sumter County: Southeastern Geology, v. 36, p. 35-46.

Smith, A.B., Jeffery, C.H., 2000. Maastrichtian and Palaeocene echinoids: a key to world faunas: Special Papers in Paleontology no. 63, The Palaeontological Association, London, 406 p.

Sohl, N. F.; Owens, J. P., 1987, Cretaceous stratigraphy of the Carolina Coastal Plain, in J. W. Horton, J., and Zullo, V. A., eds.: The Geology of the Carolinas; Carolina Geological Society Fiftieth Anniversary Volume, The University of Tennessee Press, Knoxville, p. 251-262.

Swift, D.J.P., 1964, Origin of the Cretaceous Pee Dee Formation of the Carolina Coastal Plain: Doctoral Dissertation, University of North Carolina, Chapel Hill. Chapel Hill, NC. p. 151.

Swift, D.J.P., and Heron, S. Duncan, Jr., 1969, Stratigraphy of the Carolina Cretaceous: Southeastern Geology, v. 10 issue 4, p. 201-245.

Wagner, C.D., 1972, A new Paleocene phymosomatoid echinoid from Baja California: Journal of Paleontology, v. 46, p. 651-655.

Wheeler, W.H., and Curran, H.A., 1974, Relation of Rocky Point Member (Peedee Formation) to Cretaceous-Tertiary boundary in North Carolina: American Association of Petroleum Geologists Bulletin, v. 58, no. 9, p. 1751-1757.

Wingard, G.L., 1993, A detailed taxonomy of Upper Cretaceous and lower Tertiary Crassatellidae in eastern North America; an example of the nature of extinction: U.S. Geological Survey Professional Paper, 1535, 131 p.